Evaluation of global wind power

Cristina L. Archer and Mark Z. Jacobson

Department of Civil and Environmental Engineering, Stanford University, Stanford, California, USA

[1]   The goal of this study is to quantify the world's wind power potential for the first time from data. Wind speeds are calculated at 80 m, the hub height of modern, 77-m diameter, 1500 kW turbines. Since relatively few observations are available at 80 m, the Least Square extrapolation technique is utilized and revised here to obtain estimates of wind speeds at 80 m given observed wind speeds at 10 m (widely available) and a network of sounding stations. Tower data from the Kennedy Space Center (Florida) were used to validate the results. Globally, $\sim$13% of all reporting stations experience annual mean wind speeds $\geq$ 6.9 m/s at 80 m (i.e., wind power class 3 or greater) and can therefore be considered suitable for low-cost wind power generation. This estimate is believed to be conservative. Of all continents, North America has the largest number of stations in class $\geq$ 3 (453), and Antarctica has the largest percent (60%). Areas with great potential are found in northern Europe along the North Sea, the southern tip of the South American continent, the island of Tasmania in Australia, the Great Lakes region, and the northeastern and northwestern coasts of North America. The global average 10-m wind speed over the ocean from measurements is 6.64 m/s (class 6); that over land is 3.28 m/s (class 1). The calculated 80-m values are 8.60 m/s (class 6) and 4.54 m/s (class 1) over ocean and land, respectively. Over land, daytime 80-m wind speed averages obtained from soundings (4.96 m/s) are slightly larger than nighttime ones (4.85 m/s); nighttime wind speeds increase, on average, above daytime speeds above 120 m. Assuming that statistics generated from all stations analyzed here are representative of the global distribution of winds, global wind power generated at locations with mean annual wind speeds $\geq$ 6.9 m/s at 80 m is found to be $\sim$72 TW ($\sim$54,000 Mtoe) for the year 2000. Even if only $\sim$20% of this power could be captured, it could satisfy 100% of the world's energy demand for all purposes (6995–10177 Mtoe) and over seven times the world's electricity needs (1.6–1.8 TW). Several practical barriers need to be overcome to fully realize this potential.

1. Introduction

[2]   The globally averaged growth rate of wind power has been 34% per annum during the past five years. As such, wind is not only the fastest growing renewable energy technology, but also the fastest growing electric power source [*AWEA*, 2004; *EIA*, 2004]. Globally, installed wind capacity at the end of 2003 was about 39,000 MW (39,000 $\times$ 10^6 W), with 14,609 MW in Germany (37%), 6374 MW in the United States (16%), 6202 MW in Spain (16%), and 3110 MW in Denmark (8%). Wind currently supplies 20% and 6% of Denmark and Germany electric power, respectively [*AWEA*, 2004].

[3]   Although the cost of wind energy has decreased substantially during the last couple of decades [*AWEA*, 2004; *Bolinger and Wiser*, 2001; *Jacobson and Masters*, 2001] and the growth rate of installed power is high,

its share of total energy is very low. In fact, wind energy produces only about 0.54% of the world's electric power [*EIA*, 2004]. The two main barriers to large-scale implementation of wind power are: (1) the perceived intermittency of winds, and (2) the difficulty in identifying good wind locations, especially in developing countries. The first barrier can be ameliorated by linking multiple wind farms together. Such approach can virtually eliminate low wind speed events and thus substantially minimize wind power intermittency [*Archer and Jacobson*, 2003]. The benefits are greater for larger catchment areas, as the spatial and temporal correlation of wind speeds is substantially reduced. For example, *Czisch and Ernst* [2001] showed that a network of wind farms over parts of Europe and Northern Africa could supply about 70% of the entire European electricity demand. Even when costs of transmission and storage are included, they estimated that the cost of wind power would not exceed 5 c/kWh. This paper focuses on the second issue, i.e., optimal siting. Global maps of wind potential at 80 m will be derived via

a revised version of the Least Square (LS hereafter) methodology [*Archer and Jacobson*, 2003]. Results will be used to obtain an estimate of the global wind power potential.

2. Methodology

[4] Wind speed and temperature data from NCDC (National Climatic Data Center) [*NCDC*, 2004] and FSL (Forecast Systems Laboratory) [*FSL*, 2004] for the years 1998–2002 were used to generate maps and statistics to examine global wind power in 2000. Two types of data were considered: measurements from 7753 surface stations and from 446 sounding stations. (Even though data were available from 490 soundings and 8071 surface locations, only stations with at least 20 valid readings in a year were utilized in this study.) Of the 446 sounding stations, 414 reported some measurements at an elevation of 80 m ± 20 m above the ground. Of all the measurements reported below 200 m (and above 20 m), ∼28% were at 80 ± 20 m. Surface stations (including buoys) provided daily averaged wind speed measurements only at a standard elevation of ∼10 m above the ground (V10 hereafter).

[5] To obtain estimates of wind speed at 80 m (V80 hereafter) at all sites (i.e., sounding, surface, and buoy stations), a revised version of the Least Square methodology is introduced. In brief, the LS methodology involves three steps:

[6] 1. For each sounding station, six possible fitting curves (described shortly) are calculated from the observed profile to reproduce empirically the wind speed variation with height at the sounding. The "best" fitting curve (i.e., the one that gives the lowest total error between calculated and observed wind speed values) is then identified and the LS parameter(s) necessary to obtain such curve is (are) saved.

[7] 2. For each surface station, the five nearest-in-space sounding stations are selected. Then, V10 from the surface station and the "best" fitting parameter(s) from each of the five sounding station are used to calculate five estimates of V80 at the surface station.

[8] 3. Finally, V80 at the surface station is calculated as the weighted average of the five new V80s from Step 2, where the weighting is the inverse square of the distance between the surface station and each sounding station.

[9] These steps are then repeated for each hour of available data. Originally, four fitting curves were introduced in *Archer and Jacobson* [2003], specifically:

[10] 1. LS log-law:

$$V(z) = V_R \frac{\ln\left(\frac{z}{z_0}\right)}{\ln\left(\frac{z_R}{z_0}\right)}, \tag{1}$$

to be used with the LS roughness length z_0^{LS}:

$$\ln\left(z_0^{LS}\right) = \frac{V_R\left\{\sum_{i=1}^{N}[\ln(z_i)]^2 - \ln(z_R)\sum_{i=1}^{N}\ln(z_i)\right\} - \ln(z_R)\sum_{i=1}^{N}\left[V_i\ln\left(\frac{z_i}{z_R}\right)\right]}{\left\{V_R\sum_{i=1}^{N}\ln(z_i) - \sum_{i=1}^{N}\left[V_i\ln\left(\frac{z_i}{z_R}\right)\right] - NV_R\ln(z_R)\right\}}. \tag{2}$$

[11] 2. LS power-law:

$$V(z) = V_R\left(\frac{z}{z_R}\right)^a, \tag{3}$$

to be used with LS friction coefficient α^{LS}:

$$\alpha^{LS} = \frac{\sum_{i=1}^{N}\ln\left(\frac{V_i}{V_R}\right)\ln\left(\frac{z_i}{z_R}\right)}{\sum_{i=1}^{N}\ln\left(\frac{z_i}{z_R}\right)^2}. \tag{4}$$

[12] 3. Two-parameter log-law (to be used when V_R is zero) of the form:

$$V(z) = A + B\ln z, \tag{5}$$

with parameters:

$$B = \frac{N\sum_{i=1}^{N}[V_i\ln(z_i)] - \sum_{i=1}^{N}V_i\sum_{i=1}^{N}\ln(z_i)}{N\sum_{i=1}^{N}\left[\ln(z_i)^2\right] - \left(\sum_{i=1}^{N}\ln(z_i)\right)^2}$$

$$A = \frac{\sum_{i=1}^{N}V_i - B\sum_{i=1}^{N}\ln(z_i)}{N} \tag{6}$$

[13] 4. Two-parameter linear profile (when wind speed decreases with height) of the form:

$$V(z) = C + Dz \tag{7}$$

with parameters:

$$D = \frac{\sum_{i=1}^{N}V_i - NV_R}{\sum_{i=1}^{N}z_i - Nz_R} \qquad C = V_R - Dz_R. \tag{8}$$

The formulation for D, different from that in *Archer and Jacobson* [2003], was obtained by imposing the passage through point z_R first, and then deriving the LS slope.

[14] In these equations, $V(z)$ is wind speed at elevation z above the ground (also represented as V_i when retrieved at point i ($i = 1...N$, $N = 3$) of the sounding profile at elevation z_i, for $z_N < 1000$ m), z_R is the reference elevation (in most cases 10 m), and V_R is wind speed retrieved at height z_R (also denoted as V10); α and z_0 are friction coefficient and roughness length respectively. The subscript LS indicates a value obtained with the LS methodology. Details of the derivation of these curves can be found in *Archer* [2004].

[15] In this study, two new fitting curves are introduced. The first one, a forced power-law, is only used when the second point of the sounding profile z_2 is above 80 m and the LS estimate of V80, obtained with one the four previous fitting curves, is larger than V_2, the observed wind speed at z_2, which would be unrealistic. A power-law profile is then

forced through three points: 0 m, z_R, and z_2; V80 obtained with this curve is thus always smaller than V_2 by design. The estimate of V80 is thus calculated from equation (3) as:

$$\frac{V80}{V_R} = \left(\frac{80}{z_R}\right)^\alpha, \tag{9}$$

where α is the friction coefficient obtained by forcing equation (3) to pass through z_2 and then solving for α:

$$\alpha^{PL} = \frac{\ln\left(\frac{V_2}{V10}\right)}{\ln\left(\frac{z_2}{10}\right)}. \tag{10}$$

[16] When the sounding profile was almost constant with height above z_2, but it had a relatively sharp increase of wind speed with height below z_2, the best fit was usually the LS log-law curve, because it reached an asymptotic value more rapidly than any other LS curve. However, it also created, at times, too much shear in the lower part of the profile and consequently an overestimate of V80. To prevent such overestimate, a new curve is introduced in this study, namely a forced linear profile, to be used only when these conditions are verified:

$$\gamma_{BOTTOM} = \frac{V_2 - V_1}{z_2 - z_1} \geq 5 \times 10^{-2} \; kt\,m^{-1} \tag{11}$$

$$-1 \leq \gamma_{TOP} = \frac{V_3 - V_2}{z_3 - z_2} \leq 2 \times 10^{-2} \; kt\,m^{-1}, \tag{12}$$

and when the estimate of V80, obtained from:

$$V(z) = E + F(z - z_R) \tag{13}$$

$$E = V_1 = V_R = V10 \qquad F = \gamma_{BOTTOM}, \tag{14}$$

is lower than that obtained with any other LS fit.

[17] With a simplified notation, the LS methodology is a function L (one among equations (1), (3), (5), (7), (9), or (13)) such that, when applied to V_R, it returns the best estimate of V80 at the station of interest, given the LS parameters obtained at a nearby sounding station. If K is the number of nearby soundings ($K = 5$ in this study), then:

$$V80 = \frac{1}{\sum\limits_{k=1}^{K} \frac{1}{R_k^2}} \times \sum_{k=1}^{K} \frac{1}{R_k^2} L_k(V_R), \tag{15}$$

where R_k is the radius of distance between the surface station and a nearby sounding station k.

[18] Other changes to the LS methodology include stricter quality control checks. Such checks were imposed with the overall goal of obtaining conservative results, even if it implied lower accuracy. V10 values were rejected when >25 m/s. V80 was accepted only if ≤3*V10 (except when V10 was zero), or, in other words, if the shear ρ = V80/V10 ≤ 3. Values of the LS parameters were retained only if realistic, as determined from data in

Jacobson [1999]. In particular, the upper limits were 0.53 for the friction coefficient and 3.5 m for the surface roughness. Note that wind direction is not used in the LS methodology. Although changes of wind direction with height might affect some of the results, this effect is not expected to be significant, especially over the 77-m span of the turbine blades considered here.

3. Results

[19] In this section, several types of analyses are discussed. First, the LS methodology is applied to all sounding stations to generate LS parameters, which are then applied to surface stations to generate global statistics of wind speed at 80 m. Second, the LS methodology performance is evaluated by comparing calculated vs. observed wind profiles at the sounding and surface stations, and at a network of 23 towers around the Kennedy Space Center (KSC), Florida. Finally, a technique of calculating global wind power is presented.

3.1. Global Spatial Distributions

[20] Five years of wind data were available for this study. Most statistics, though, were applied only to the year 2000 to be consistent with *Archer and Jacobson* [2003]. The year 2000 is fairly representative of the 5-year period 1998–2002. As shown in Figure 1a, the global average of wind speed in 2000 at any level was within −0.6 and +1.6% of the 5-year average at that level; the near-surface mean wind speed in 2000 was within less than 0.25% of the five-year average. The profiles of temperature and dew point temperature, shown for completeness in Figures 1b and 1c, suggest that the year 2000 was slightly cooler and drier than the five-year average. These figures were obtained by averaging sounding measurements retrieved at a pressure of ±20 hPa of each mandatory value from 429 stations with valid readings during all five years. Note that these global profiles are inevitably biased towards mid-latitudes since more sounding stations are found in the mid-latitudes than anywhere else.

[21] The globally averaged profiles of wind speed, temperature, and dew point during day and night for the year 2000 are shown in Figure 1d. Wind speed was lower during the day than at night at all levels, whereas temperature and dew point were greater during the day than at night, except at the 200–100 hPa level, where no significant difference was found. The jet stream is clearly located between 300 and 200 hPa, where wind speed is maximum. The tropopause is located at about 100 hPa, where temperature and dew point start to increase with height.

[22] Figure 2 shows the world map of V80 obtained with the LS methodology at sounding locations with 20 or more valid readings for the year 2000. To the authors' knowledge, this is the first map of 80-m wind power for the world published to date. The spatial coverage is excellent over the U.S., southern Canada, and Central Europe; good over eastern China, western Russia, and coastal Australia; Africa and Antarctica are the worst represented continents, especially in the interior.

[23] The map shows that the majority of the stations belong to class two or lower (90%, Table 1). Many locations with appreciable wind power potential, i.e., class 3 or
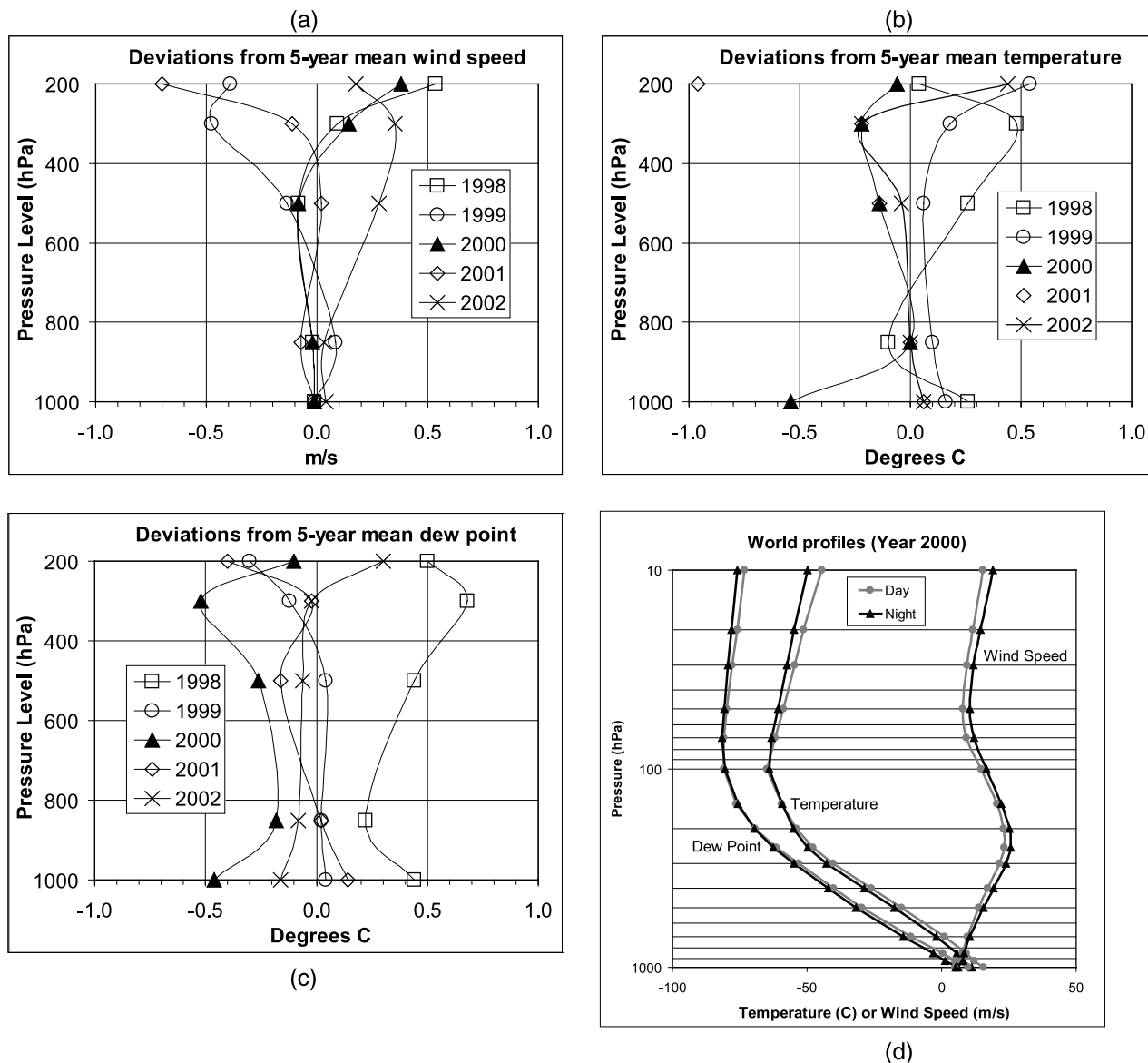
(a)

(b)

(c)

(d)

Figure 1. Vertical global profiles of: differences between 2000 and 5-year average of (a) wind speed, (b) temperature, and (c) dew point temperature; (d) average temperature, dew point temperature, and wind speed (day and night) for the year 2000.

greater, are located near coasts, such as in Alaska and northern Europe. Overall, the application of the LS methodology to the world shows that 10.1% of the sounding locations belong to class 3 or greater at 80 m (Table 1) and are therefore suitable for wind power generation.

[24] Figure 3 shows the world map of V10 observed at all sounding locations with 20 or more valid readings. This map can be used to evaluate the world 80-m map (Figure 2) because there should be a correlation between windy locations at the surface and windy locations at 80 m. In fact, the two maps show generally the same distribution of wind power class (e.g., South-East Asia and Australia). Wind shear, however, can vary at locations with similar surface conditions, and thus generate differences in wind classes at 80 m. As shown in Table 1, 75.6% (75.4%) of the sounding stations fell in class 1 at 80 m (10 m). Fewer stations fell in class 3 or greater at 80 m (10.1%) than at

10 m (14.7%), suggesting that the LS methodology might be conservative when applied directly to vertical profiles (Step 1 above). Note that more stations are shown at 10 m (570) than at 80 m (446) because not all sounding stations retrieve a complete vertical profile of winds.

[25] Wind shear can be evaluated further in Table 2, which shows the number of stations that stayed in the same class at 80 m and at 10 m ($Class_{80} = Class_{10}$), moved up ($Class_{80} > Class_{10}$), or moved down ($Class_{80} < Class_{10}$) among the 446 sounding stations for each 10-m class. In 75.3% of the cases, a sounding station was found to offer the same wind power potential at 80 m as it did at 10 m. This suggests that, to a first approximation, a station with good potential at 10 m offers also a good potential at 80 m. However, for a given wind power class at 10 m, the LS methodology was more likely to estimate a lesser than a greater wind power class at 80 m (17.9% versus 6.7%
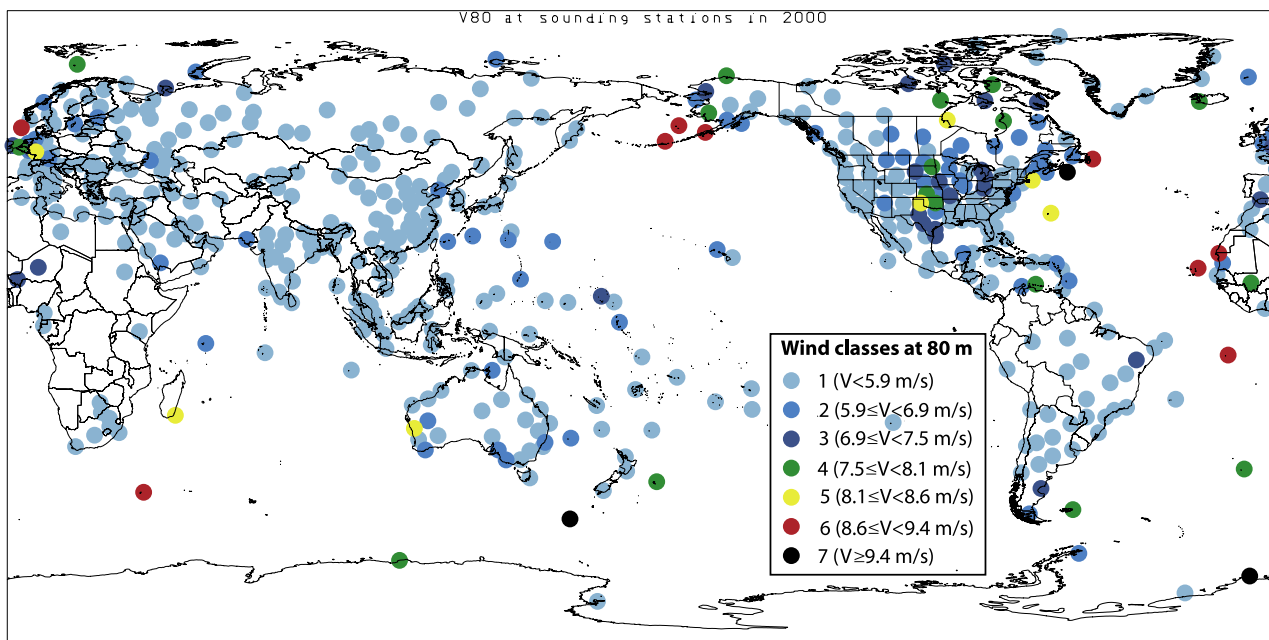
Figure 2. Map of wind speed extrapolated to 80 m and averaged over all days of the year 2000 at sounding locations with 20 or more valid readings for the year 2000.

respectively). This, again, is indicative of a conservative approach.

[26] When applied to the 7753 surface stations (Steps 2 and 3), the LS methodology produced similar results to those obtained for the sounding stations in terms of percentages in each wind power class. From Table 1, about 76% of the surface stations were in class 1 and ~13% offered appreciable wind power potential at 80 m (class 3 or greater). However, this value was slightly larger than that at 10 m (12.1%), the opposite of what was found for sounding stations. In fact, the application of the LS methodology to surface stations was more likely to predict a move up (10.6%) than a move down (6.9%) at 80 m for a given 10-m class (Table 2). This finding could potentially compromise the conservative nature of the methodology and will be analyzed in detail in the next section.

[27] Since a map of V80 at 7753 surface and 446 sounding stations analogous to Figure 2 is difficult to read, results will be shown for the following regions: Europe,

Australia, South America, North America, South-East Asia, North-Central Asia, and Africa. Comparison with previous work is limited to published studies and to reports freely available to the public.

[28] The map of Europe is shown in Figure 4. A previous European map was created by *Troen and Petersen* [1989] (available at http://www.windpower.org/en/tour/wres/euromap.htm). Both maps show that the greatest potential in Europe is along northeastern coasts, particularly in France, Belgium, Netherlands, Germany and Denmark. The coasts of the United Kingdom and the islands in the North Sea have stations mainly in class 7 too. However, the present study did not find class 7 potential over the Scandinavian Peninsula and Ireland; this study also offers results for Eastern Europe. A wind atlas for the Baltic region was developed by *Rathmann* [2003], but at 50 m above ground and for a constant roughness length of 0.10 m. Figure 4 shows that Slovakia and the Czech Republic have several locations in class 7, but none is found in Austria or Russia (except along the northern coast). Table 3 shows that

Table 1. Number and Percent of Stations in Each Wind Power Class at Both 80 and 10 m for the Year 2000 at Sounding, Surface, and All Locations Worldwide With at Least 20 Valid Measurements[a]

	Sounding Stations				Surface Stations				All Stations			
	V80		V10		V80		V10		V80		V10	
Class	Count	Percent	Count	Percent	Count	Percent	Count	Percent	Count	Percent	Count	Percent
1	337	75.6	410	75.4	5885	75.9	6144	79.0	6222	75.9	6554	78.8
2	64	14.3	54	9.9	875	11.3	689	8.9	939	11.5	743	8.9
3	16	3.6	31	5.7	321	4.1	295	3.8	337	4.1	326	3.9
4	13	2.9	14	2.6	220	2.8	149	1.9	233	2.8	163	2.0
5	6	1.3	10	1.8	126	1.6	120	1.5	132	1.6	130	1.6
6	7	1.6	6	1.1	124	1.6	124	1.6	131	1.6	130	1.6
7	3	0.7	19	3.5	202	2.6	256	3.3	205	2.5	275	3.3
Total	446	100.0	544	100.0	7753	100.0	7777	100.0	8199	100.0	8321	100.0
Class ≥ 3	45	10.1	80	14.7	993	12.8	944	12.1	1038	12.7	1024	12.3

[a]Total number and percent of stations in class higher than 3 are listed in the last row.
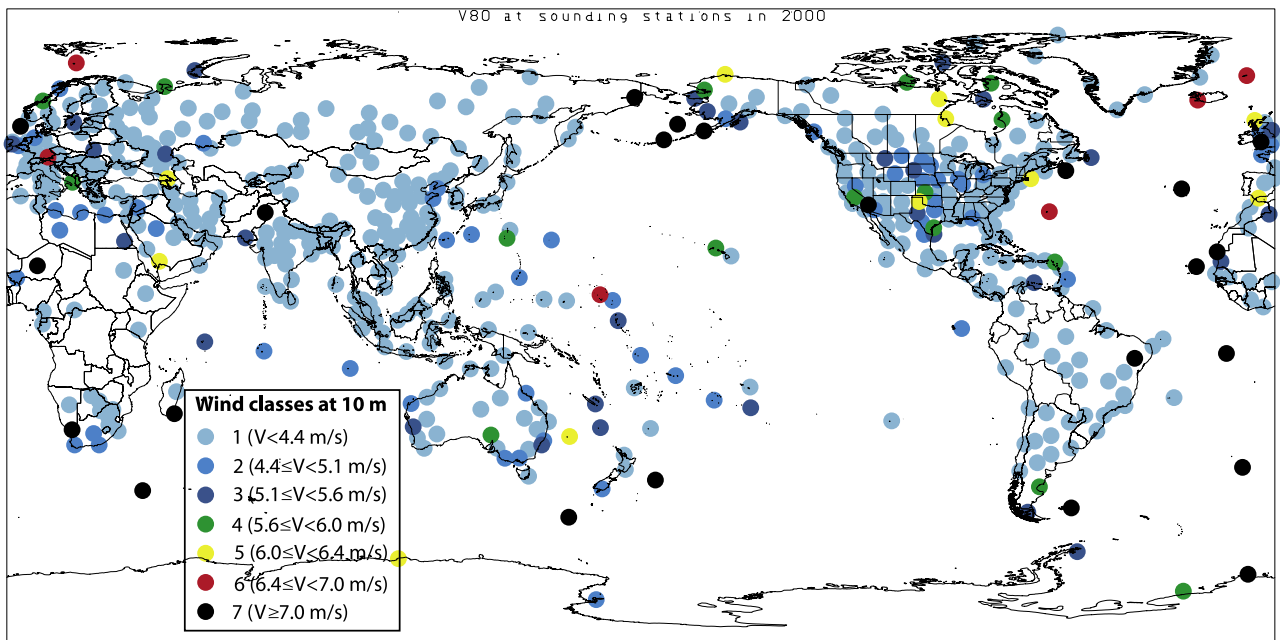
Figure 3. Same as Figure 2, but for observed wind speed at 10 m.

overall 14.2% of the European stations are in class 3 or greater. Europe also has the densest station spatial coverage of all continents, as indicated by the Coverage Index (206), calculated as the average number of stations per million km^2 of area.

[29] In South America (Figure 5), most available stations are in class ≤ 2 and are thus not suitable for wind power generation. A few exceptions are in the Caribbean Islands to the south-east of Cuba (where 13/41 stations, or 32%, were in class ≥ 3), the Antilles islands, the southern tips of Chile and Argentina, and the coastal area of Argentina between Bahia Blanca and Peninsula Valdes. Mexico presents a few isolated class ≥ 3 stations in the northeast and along the Yucatan Peninsula. Similar results were found at 50 meters by *Schwartz and Elliott* [1995]. Overall, the average wind speed in South America is 4.2 m/s (class 1), but this result should be taken with caution, as the Coverage Index is low (20 in Table 3).

[30] In Australia (Figure 6), the greatest potential is near coastal locations. All the islands in the Coral Sea belong to class 4 or higher; in Tasmania, the number of stations in class 7 (10) alone is greater than the number of stations in class 1 (6); the coastline between Melbourne and

Adelaide, and the areas to the south of Perth and Dampier have over 25 locations in class ≥ 5. Overall, Oceania has good spatial coverage (Coverage Index between 50 and 100) and an enormous potential for wind power, with 21% of stations in class ≥ 3 (Table 3).

[31] North America is shown in Figure 7. In the United States, the central belt (including North and South Dakota, Nebraska, Kansas, and Oklahoma), previously identified by *Elliott et al.* [1986], *Schwartz and Elliott* [2001], and *Archer and Jacobson* [2003], was found in this study to be one of the most promising continental areas for wind power in the world (average wind speed ~7.0 m/s, class 3). The eastern and southern coasts offer good potential as well, especially offshore. A new finding is the area of the Great Lakes, where the average wind power class is 6 (8.46 m/s), a wind potential shared by U.S. and Canada. Both coasts of Canada show a high number of class 7 stations (17 on the east and 7 on the west), especially around the Vancouver and Newfoundland Islands. High-resolution work in Canada, overall consistent with Figure 7, is in progress by the Canadian Meteorological Center and some preliminary results can be found at http://www.cmc.ec.gc.ca/rpn/modcom/eole/CanadianAtlas.html.

Table 2. Number of Sounding and Surface Stations for Which Calculated Wind Power Class at 80 m Is Equal, Greater, or Smaller Than Their Observed Wind Power Class at 10 m, Listed by 10-m Wind Power Class, for Stations With 20 or More Valid Readings

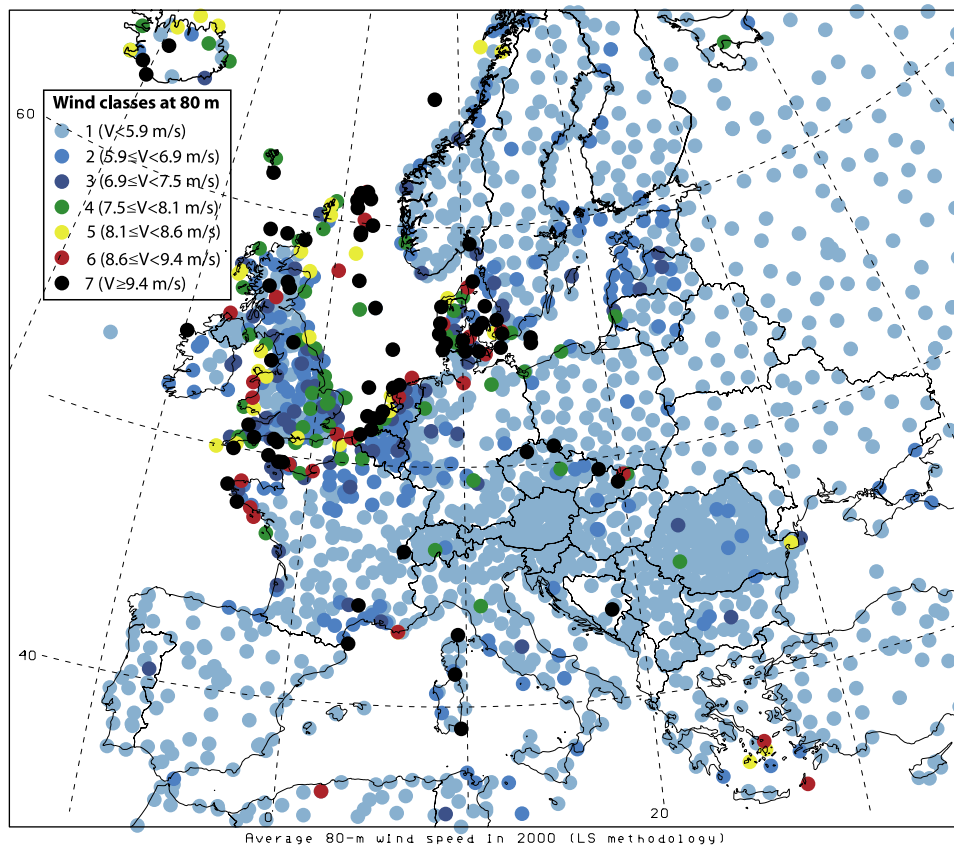|	Sounding Stations			Surface Stations		
$Class_{10}$	$Class_{80} = Class_{10}$	$Class_{80} > Class_{10}$	$Class_{80} < Class_{10}$	$Class_{80} = Class_{10}$	$Class_{80} > Class_{10}$	$Class_{80} < Class_{10}$
1	305	23	N/A	5685	441	N/A
2	20	4	25	343	171	172
3	5	3	20	88	112	95
4	2	0	12	44	43	61
5	1	0	6	26	32	61
6	0	0	5	35	25	64
7	3	N/A	12	172	N/A	83
Tot	336	30	80	6393	824	536
Percent	75.3	6.7	17.9	82.5	10.6	6.9

Figure 4. Map of wind speed extrapolated to 80 m and averaged over all days of the year 2000 at surface and sounding stations with 20 or more valid readings in Europe.

[32] Figure 8 shows the map of 80-m wind power for Asia. The majority of this area is not suitable for wind power generation. Over the entire territories of India, Malaysia, Indonesia, and Philippines, for example, not a single station was in class 3 or higher! Note that several areas with wind power density of 300 W/m^2 or more at 50 meters have been identified in India in a study available at http://www.windpowerindia.com/statwind.html in 2003. *Elliott et al.* [2002] found that about 23% of the land in Southeast China was in class ≥ 3, whereas for the same area only 12% (i.e., 1 station in class ≥ 3 out of 8) was found in this study. The only countries with appreciable wind potential are Japan (9% of the stations in class ≥ 3), a few islands in the China Sea (e.g., Taiwan), and the Guam and Mariana Islands (both U.S. territories). Results for Southeast Asia are generally in agreement with *ASTAE* [2001], i.e., poor potential on over 80% of the territory. Vietnam, however, was classified as class 1 in this study but it was shown to have good (7–8 m/s) to excellent (>9 m/s) wind power potential on over 8% of its territory at 65 meters [*ASTAE*, 2001]. The disagreement can be attributed to the lack of measurements in such areas, which are therefore not represented in the current study. A few locations along the northeastern coast of Russia, however, offer great potential:

Table 3. Number and Percent of Sounding and Surface Stations (With at Least 20 Valid Readings in Year 2000) in Each Wind Power Class at 80 m and Coverage Index, Calculated as the Ratio Between Number of Stations and Continent Area, Listed by Continents

| Class	Europe N.	Europe %	North America N.	North America %	South America N.	South America %	Oceania N.	Oceania %	Africa N.	Africa %	Asia N.	Asia %	Antarctica N.	Antarctica %
1	1586	73.3	1473	61.8	305	84.3	402	64.2	521	91.7	1910	93.7	18	32.7
2	271	12.5	458	19.2	22	6.1	91	14.5	21	3.7	73	3.6	4	7.3
3	83	3.8	165	6.9	14	3.9	38	6.1	8	1.4	26	1.3	3	5.5
4	78	3.6	111	4.7	5	1.4	24	3.8	4	0.7	12	0.6	3	5.5
5	32	1.5	68	2.9	3	0.8	15	2.4	5	0.9	7	0.3	2	3.6
6	36	1.7	48	2.0	6	1.7	25	4.0	4	0.7	4	0.2	7	12.7
7	78	3.6	61	2.6	7	1.9	31	5.0	5	0.9	6	0.3	18	32.7
Total	2164	100.0	2384	100	362	100	626	100	568	100	2038	100	55	100
Total classes ≥ 3	307	14.2	453	19.0	35	9.7	133	21.2	26	4.6	55	2.7	33	60.0
Surface[a] ($\times 1000$ km^2)	10498		24238		17835		8502		30335		43608		13209	
Coverage Index	206		98		20		74		19		47		4	

[a]World Atlas, DK, New York, 1999.
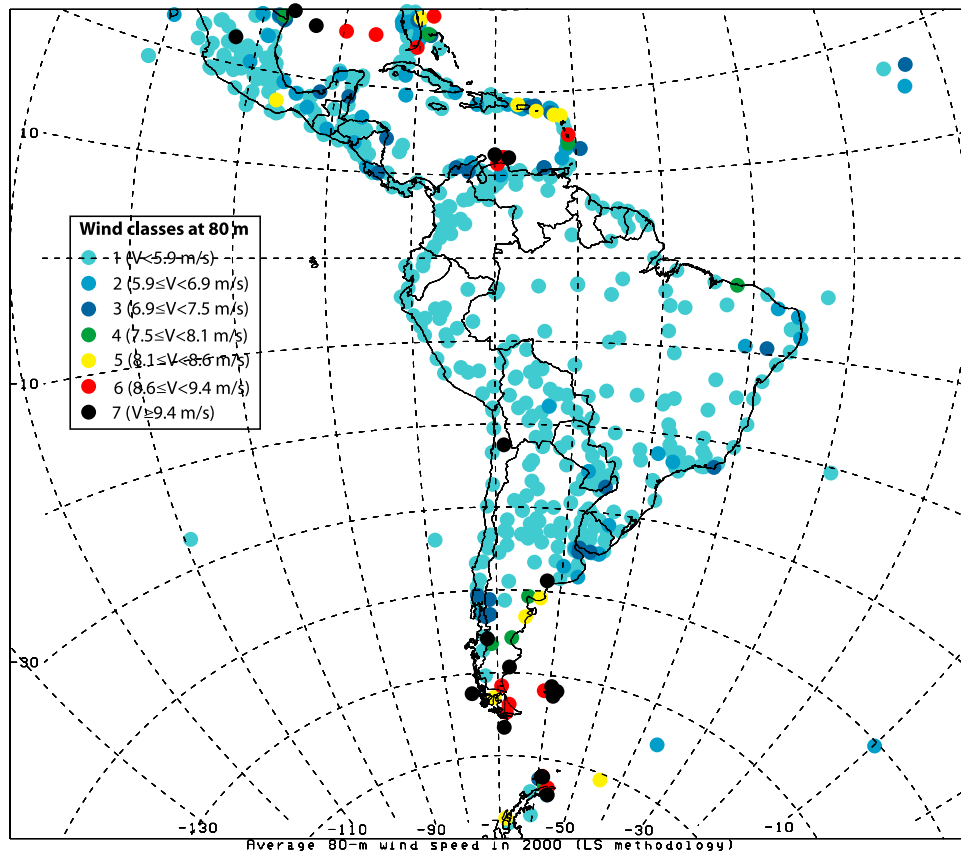
Figure 5. Same as Figure 4, but for South America.

Cape Uelen (class 5), Dikson Island (5), Malye Karmakuly (7), and Vize Island (5). This area was also identified in a 2001 wind resource study at 50 m for Russia available at http://www.inforse.dk/europe/windrus.htm. A Russian wind atlas was developed by *Starkov et al.* [2000], but it was not publicly available.

[33] Finally, the map of Africa is shown in Figure 9. The coverage of surface stations is better than that of radiosonde stations, but it is still low (Coverage Index lower than 25 in Table 3). The sparseness of sounding stations resulted in the utilization of fitting parameters that were not always representative of the area of the surface station of interest. In fact, no threshold on the radii of influence of sounding stations (used in Step 3) was imposed, in order to maximize the number of stations used. Thus, the results for this continent should be viewed with caution for this reason. Good potential is present in the Canary Islands (Spain) to the west, the Ascension Island (U.K.) in the Atlantic Ocean, and in a few isolated stations in Madagascar, South Africa, Kenya, Ethiopia, and the Socotra Island (Yemen) to the East.

[34] One last aspect under investigation was the potential for offshore wind farm development. The main advantage of offshore siting is reduced surface roughness, which results in higher wind speed and thus greater wind power production. Also, the strength of the horizontal thermal gradient is maximum near the shore. Data from 81 buoys/ platforms were available from NCDC; they were located along the coasts of United States (51), Canada (8), and the United Kingdom (22). Over 60% of these buoys had

average wind speeds at 80 m in the highest wind power classes (6 and 7). The average 80-m wind speed for the 75 out of 81 offshore sites with at least 20 valid readings in the year 2000 (Table 4) was 8.60 m/s (class 6); if only locations in class ≥ 3 were included, the 80-m mean wind speed was 9.34 m/s (class 6). By comparison, over land the average wind speed at 80 m was 4.54 m/s (class 1), whereas for stations in class ≥ 3 it was 8.40 m/s (class 5). In other words, a wind farm located offshore could experience wind speeds that are, on average, 90% greater than wind speeds at a wind farm located over land. When all land (surface and sounding) and offshore sites were included, the global average wind speed at 80 m was 4.59 m/s (8.44 m/s for class ≥3 sites).

3.2. Validation

[35] Of the three steps involved in the LS methodology, Step 1 deals directly with the sounding data, while Steps 2 and 3 involve the application of the LS fitting parameters to the surface stations. The validation of the LS methodology will thus be divided in two parts. Part 1 will focus on sounding stations, to evaluate the correctness of extrapolating V80 from observed vertical profiles with the LS parameters. Part 2 will focus on surface stations, to evaluate the correctness of Steps 2 and 3. As mentioned in the previous section, it is more likely that a surface station will belong to a higher class at 80 m than at 10 m when the LS methodology is used. As such, the conservative nature of Steps 2 and 3 could be questionable. Wind speed data from a network of 23 towers around the Kennedy Space Center
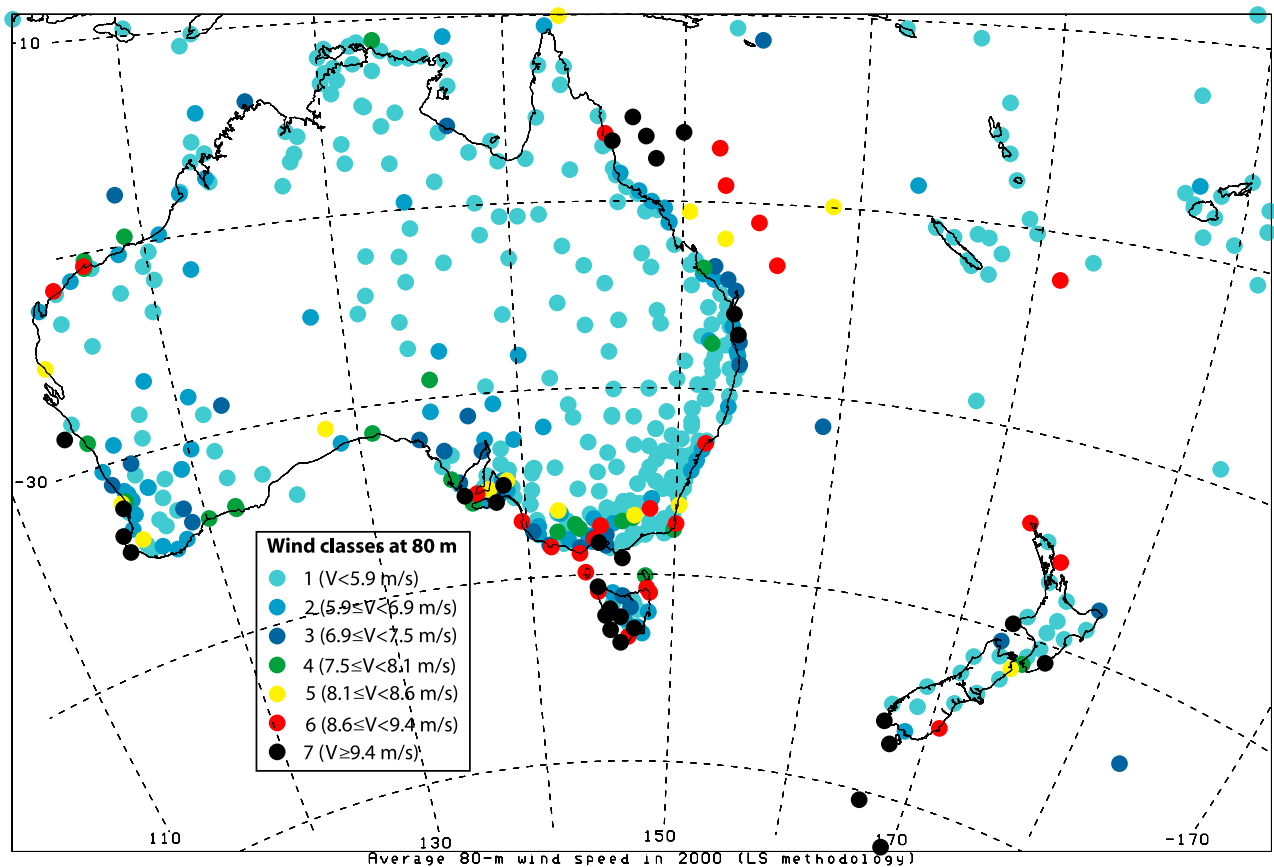
Figure 6. Same as Figure 4, but for Australia.

(KSC), Florida, obtained from the Applied Meteorology Unit (AMU) and the KSC Weather Office, were utilized to confirm the results.

3.2.1. Part 1: Sounding Stations

[36] First, observed profiles with at least three points below 1000 m were divided into six groups, according to which of the six LS fitting curves had the lowest residual. Next, the data were subdivided into "Day" and "Night", depending on whether the profile was retrieved during day or night. Such classification was performed based on geographical and astronomical parameters (such as latitude, longitude, and station elevation, which permitted the determination of solar declination, mean anomaly, ascension, and true longitude), and not on political time zones. The global-mean value of each fitting parameter (diurnal and nocturnal) was then determined and compared with observed profiles and with other global statistics.

[37] Figure 10 shows all the observed sounding profiles worldwide in the lowest 300 m for which, for example, the best fitting curve was the Log-law with LS roughness length (equation (1)). Analogously, profiles for which the best fitting curve was the Power-law with LS friction coefficient (equation (4)) are presented in Figure 11. In both cases, the globally averaged V80 values from the power- and log-laws with LS parameters (triangle) were greater than those obtained by using the constant-coefficient log- or power-laws (with benchmark values of $z_0 = 0.01$ m and $\alpha = 1/7$ respectively), both during day and night. This was generally true of the other fitting curves too, with the exception of the LS linear profile, which by design produced estimates of

V80 lower than the corresponding estimates by constant-coefficients log- and power-laws (not shown).

[38] The global-averages of the LS fitting parameters (shown in Table 5) were used to draw global-average fitting curves in Figure 10 and Figure 11 (solid lines), which appear to be good approximations for the data. The global-average of V80 (obtained as the arithmetic mean of daily V80^{LS} values at all stations) is generally lower than the value obtained with the global-average fitting parameters (obtained by multiplying the global-averaged observed V10 value by the arithmetic mean of each LS fitting parameter), which confirms the conservative nature of the results obtained with the LS approach.

[39] The fitting parameter values vary from day to night too (Table 5). For example, with the LS log-law, the global-average roughness length was 0.81 m at night and 0.63 m during the day. (Note that, from equation (2), as z_0 increases, wind speed increases with height above z_R; vice versa, for $z < z_R$, wind speed is lower for larger z_0. As such, nocturnal wind speed is larger than diurnal wind speed as surface roughness increases from day to night.) These values, observed for orchards, coniferous forests, and cities [*Jacobson*, 1999] are about two orders of magnitude greater than the benchmark value $z_0 = 0.01$ m (typical of grass). For the LS power-law, the global-average friction coefficient varied between 0.26 at night to 0.23 during the day; such values are greater than the benchmark value $\alpha = 1/7$ (0.14) and are more representative of urbanized areas ($\alpha \sim 0.40$) than they are of smooth surfaces ($\alpha \sim 0.10$). This suggests that, in the absence of any other information, the LS values
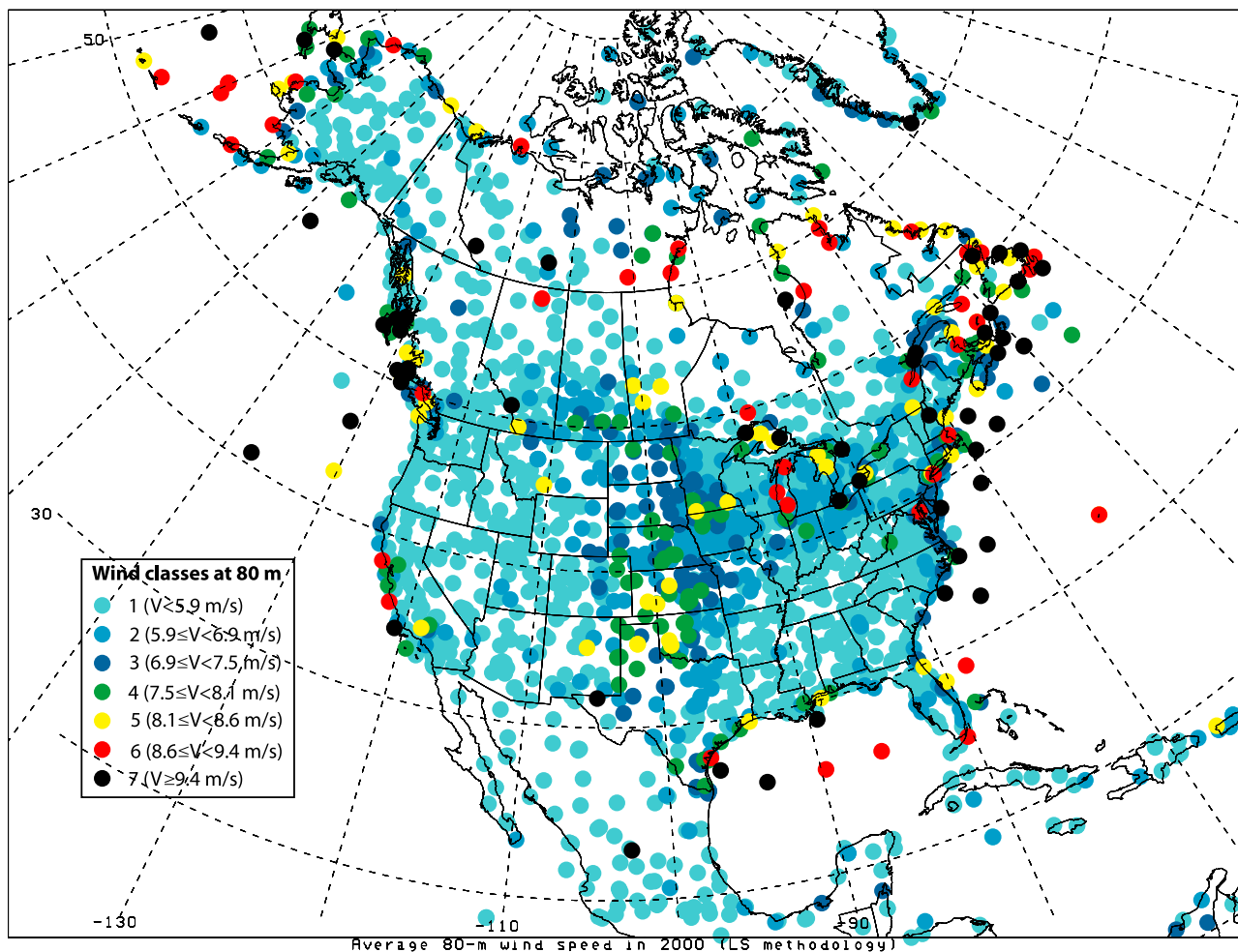
Figure 7. Same as Figure 4, but for North America.

in Table 5 are a more realistic "first guess" to calculating wind speed profiles (e.g., in numerical modeling studies with vertical resolution of the order of 100 m) than are the constant coefficients $\alpha = 0.14$ and $z_0 = 0.01$ m. It also confirms that, on average, the data used in this study are more representative of urbanized areas than they are of wild regions.

[40] Table 5 also shows a comparison between the average LS value of V80 and the average observed value of V80 from sounding stations that retrieved wind speed data at an elevation of 80 ± 20 m (V80^{OBS}). Even though the number of such observations is smaller ($\sim$6%) than the total number of sounding observations below 300 m, and therefore the significance of this comparison is uncertain, it shows that the LS estimates are excellent (e.g., the LS averages were within -15% and $+26\%$ of the corresponding observed ones). In most cases (i.e., LS log-law, LS linear, two-parameter LS log-law, and forced linear), the LS curves perform better than both the constant-coefficient log- and power-law (V^{LOG} and V^{POW}); for the forced power-law case, the three curves perform similarly. LS estimates with the LS power-law, however, appear to be higher than observed V80 values. This can be explained by the larger number of observations below 80 m (3219) than above 80 m (656) included in the calculation of V80^{OBS} during the day, for example. This is intrinsic of the LS power-law fitting

curve, since only profiles for which the second measurement is below 80 m were used. If the range of values used for the mean observed V80 is varied from $60-100$ m to $70-100$ m, for example, then the observed value of V80 at night becomes 5.8 m/s, closer to the LS estimate 6.1 m/s. The exact opposite applies to the forced power-law, because only profiles for which the second point above 10 m is above 80 m were used. The mean V80^{OBS} is thus likely to be larger than what it should be. If, for example, the range of elevations used is changed from $60-100$ m to $60-90$ m, the observed V80 becomes 5.62 m/s, closer to (and still greater than) its LS estimate (5.55 m/s).

[41] Globally, the average wind speed at 80 m from the soundings was slightly higher during the day (4.96 m/s, from 424 sounding stations) than it was at night (4.85 m/s, from 391 sounding stations), a somewhat surprising result (Figure 12). (The global average of wind speed at 80 m obtained at the sounding stations was 4.84 m/s in Table 4, which is lower than both the diurnal and the nocturnal averages. Since not all sounding stations report both during day and night, a given station is always counted in the global average, but it may or may not be included in the day (or night) average.) *Archer and Jacobson* [2003] had previously found that wind speed at 80 m in the U.S. was generally higher at night than it was during the day. However, that conclusion was based on a limited network
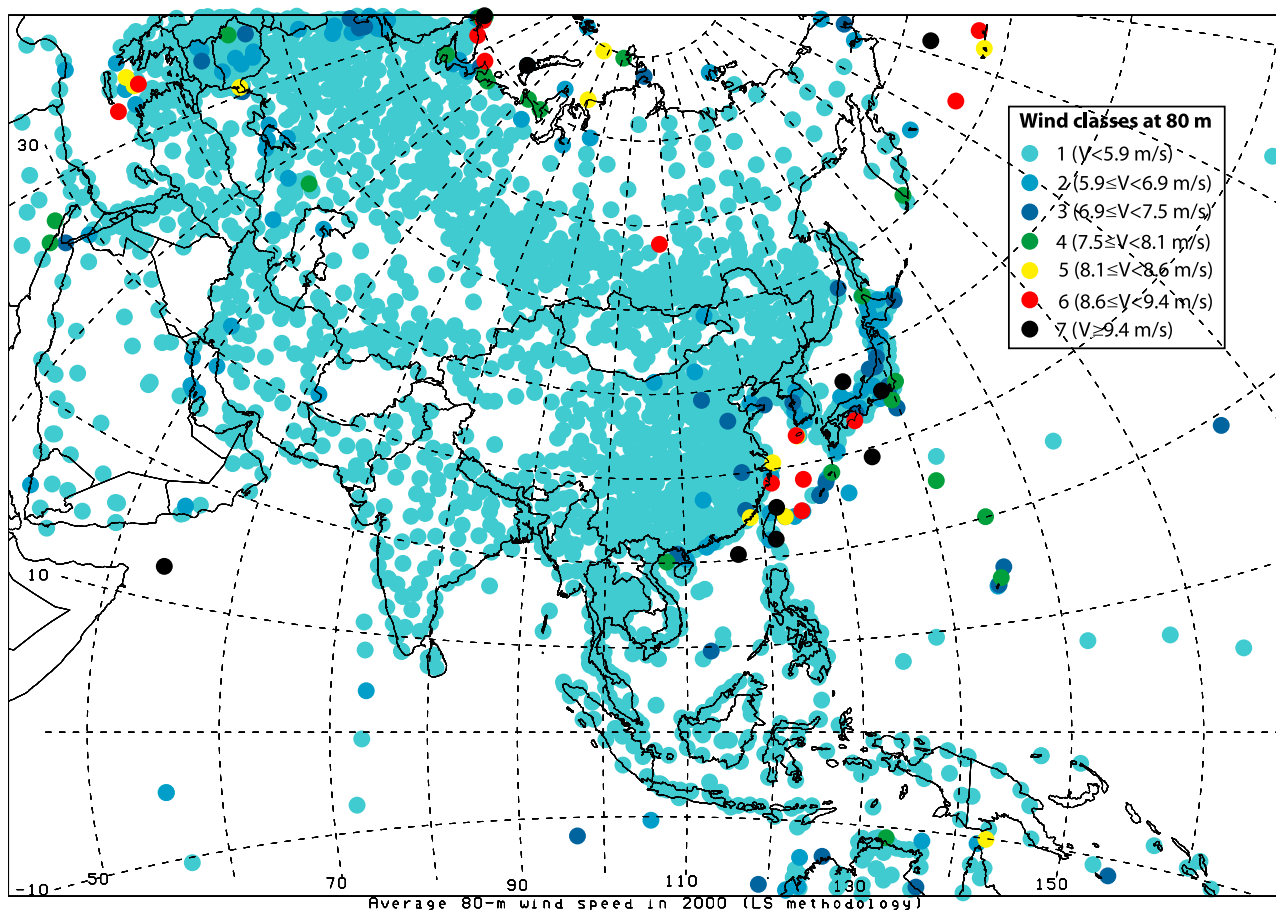
Figure 8. Same as Figure 4, but for Asia.

of ten selected stations. In this study, only the log-law curves predicted higher values of V80 at night than during the day (Table 5). All other curves showed higher values during the day than night. Note that most observations of V80 in Table 5 support this finding. After applying the LS methodology to the sounding stations for different hub heights (between 50 and 200 m), it was found that wind speed was higher at night than during the day only above 120 m (Figure 12). Near the surface, diurnal thermal instability brings momentum down from the upper levels and causes diurnal maxima of wind speed. At some level aloft z_{rev} [*Archer and Jacobson*, 2003], this trend is reversed as wind speed is minimum during the day because of the same thermally driven downward momentum fluxes. This study suggests that an average value of z_{rev} could be 120 m, the elevation at which, from Figure 12, diurnal and nocturnal average wind speeds do not differ substantially.

[42] To evaluate further the accuracy of the LS methodology, high-resolution wind speed data from a network of 44 towers around the Kennedy Space Center (KSC), Florida, were utilized. One-hour averages were calculated from the original five-minute data, to make this observational dataset as close as possible to that used in the rest of this study. Similarly, the year 2000 was selected from the available 1998–2003 year range. Of the 44 towers available, eight measured winds at four or more heights (or levels). Since at least three heights are needed to calculate the LS parameters and a measurement at one

additional height is needed for validation, these eight towers were used to validate the vertical extrapolation part of the LS methodology (Step 1) and will be indicated as "four-level towers". Fifteen towers measured winds at two heights and were used for validating Steps 2 and 3 of the LS methodology in the next section. They will be referred to as "two-level towers". Figure 13 shows the location of the KSC towers used in this study, together with the location of the sounding stations existing in the area, and Table 6 lists, for each tower, the heights with measured winds. Note that, even though the LS methodology was designed to obtain wind speed at an "output height" of 80 m given wind speed at a "reference height" of 10 m, it can be applied to any reference and/or output height. Reference and output levels are indicated in Table 6; "output height" data were not used for the calculation of the LS parameters but only for validation.

[43] Results for the four-level towers are summarized in Table 7. For all towers, whether all levels (N > 3) or only three levels (N = 3) were utilized, the LS methodology produced good estimates. The average error ε, calculated as:

$$\varepsilon = \frac{V^{LS} - V^{OBS}}{V^{OBS}} \times 100, \tag{16}$$

where V^{LS} the average wind speed obtained with the LS methodology and V^{OBS} is the average observed wind speed, was −3.0% or −3.2%, depending on whether all or only
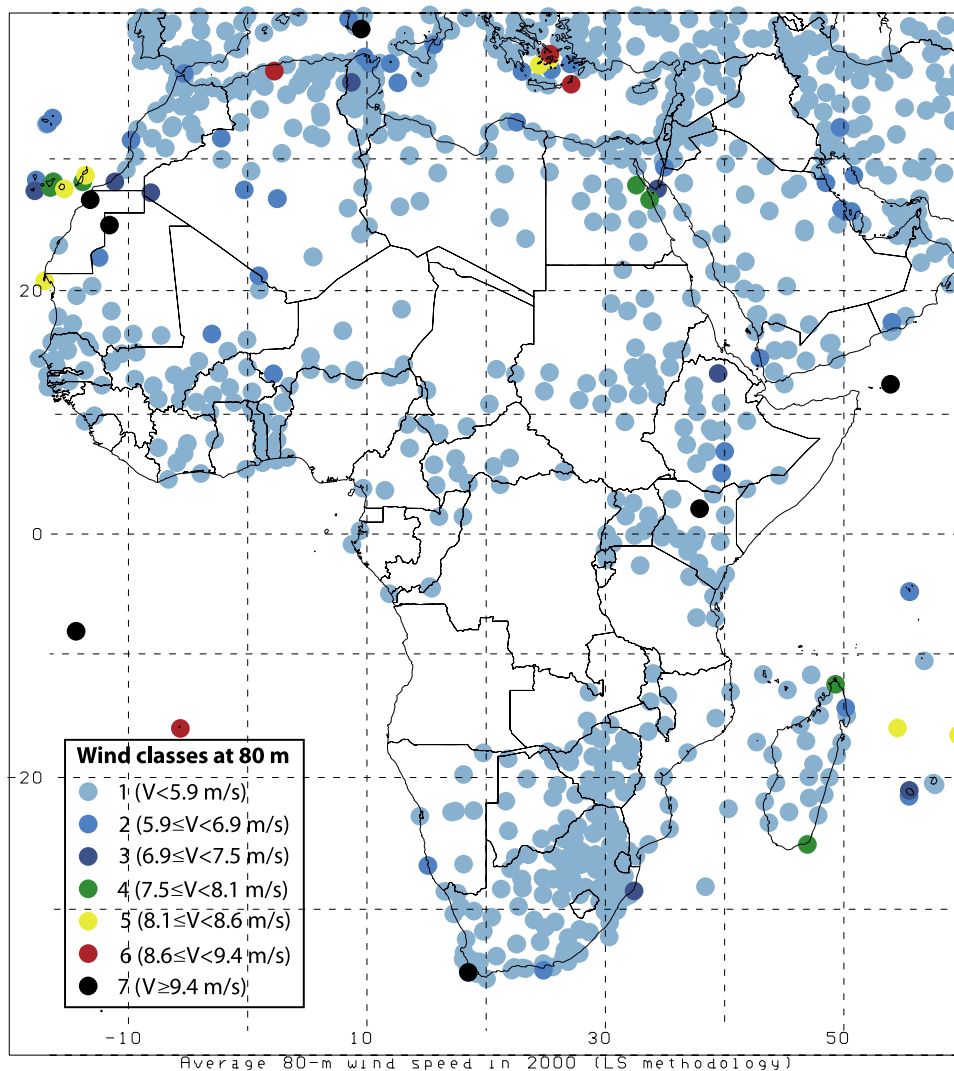
Figure 9. Same as Figure 4, but for Africa.

three levels were used. For all four-level towers, the LS results were also conservative, i.e., $\varepsilon < 0$. As expected, reducing the number of levels caused a slight deterioration of the results, but always towards more conservative estimates. For example, at tower 3131 the average error was −4.8% when six levels were used and −5.6% with only three levels. Also shown in Table 7 are the wind speed estimates obtained with the constant coefficient power- and

log-laws, V^{POW} and V^{LOG} respectively, which were in all cases worse than the corresponding LS estimates.

[44] Particular attention was devoted to extreme overestimates, defined as cases with $\varepsilon > 50\%$. The LS methodology appeared to be satisfactory, since it produced a very small number of such overestimates (between 0 and 0.24% of available profiles), all of which were characterized by unusual low-level wind speed peaks. Note that such peaks

Table 4. Mean 80-m and 10-m Wind Speeds From All Classes or From Only Classes ≥ 3 at Different Station Types (Year 2000, Only Stations With at Least 20 Valid Measurements)

Station Type	Mean V80, m/s	Mean V10, m/s	Mean V80 for Class ≥ 3 Stations, m/s	Mean V10 for Class ≥ 3 Stations, m/s
Surface over land	4.54	3.28	8.40	6.50
Buoys	8.60	6.64	9.34	7.26
Soundings	4.84 (Night: 4.85, Day: 4.96)[a]	3.31	8.02	6.26
All	4.59	3.31	8.44	6.53

[a]It may appear inconsistent that the overall average value (4.84 m/s) was lower than both the daytime (4.96 m/s) and the nocturnal (4.85 m/s) averages. The explanation resides in the different stations included in the three averaging calculations. The overall average obtained from all 446 sounding stations, the nocturnal average from 391, and the daytime average from 424.

Table 5. Statistics Obtained by Applying the Six Fitting Profiles Described in the Text to the Sounding Stations

Fitting Curves		Number of Profiles	Average Fitting Parameter(s)	V80^{LS}, m/s	V80^{POW}, m/s	V80^{LOG}, m/s	V80^{OBS}, m/s	Number of V80^{OBS}
Log-law with LS roughness length z_0^{LS}	Day	14727	0.63	5.87	5.17	5.00	6.53	2853
	Night	14001	0.81	5.88	4.91	4.75	6.95	2394
Power-law with LS friction coefficient α^{LS}	Day	23098	0.23	6.09	5.58	5.39	5.55	3875
	Night	21606	0.26	5.93	5.02	4.85	5.39	3335
Log-law with two LS parameters A and B	Day	11320	A = −2.86, B = 01.177	2.29	0.00	0.00	1.82	3441
	Night	11154	A = −2.80, B = 01.18	2.37	0.00	0.00	1.91	2450
Linear profile with LS coefficients C and D	Day	28402	C = 4.33, D = 0.001	4.40	5.84	5.65	4.07	5932
	Night	17242	C = 3.8, D = 0.002	3.98	5.14	4.97	3.81	3402
Forced power-law with friction coefficient α^{PL}	Day	12065	0.13	5.55	5.99	5.79	5.78	3737
	Night	9787	0.15	5.25	5.45	5.27	5.66	3182
Forced linear profile with coefficients E and F	Day	5001	E = 4.68, F = 0.039	7.38	6.30	6.09	7.43	556
	Night	6065	E = 4.39, F = 0.039	7.11	5.91	5.71	7.20	461

were not resolvable with the data used, since the minimum wind speed in the profile occurred at the output level, which was not used in the LS parameter calculation. Figure 14 shows the average profiles obtained at the four four-level towers (i.e., 20, 21, 3131, and 3132) and the single profile with the worst LS methodology performance for each tower. In conclusion, the KSC data from the four-level towers confirmed that the LS methodology produces both accurate and conservative results, and that three levels are adequate to extrapolate the full vertical profile of wind speed.

3.2.2. Part 2: Surface Stations

[45] Ideally, the LS methodology should be applied to simultaneous sounding and surface data. In other words, for each given hour, the LS parameters should be determined from the soundings and then applied, at the surface station, to the value of V_R valid at the same hour as the sounding profiles. The daily average of V80 at a surface station (i.e., $\overline{V}80$) should thus be calculated as follows:

$$\overline{V}80 = \frac{1}{24} \times \sum_{h=1}^{24} \frac{1}{\sum_{k=1}^{K} \frac{1}{R_k^2}} \times \sum_{k=1}^{K} \frac{1}{R_k^2} L_k^h \left(V_R^h \right), \qquad (17)$$

where L_k^h is the LS function at sounding station k at hour h, V_R^h is 10-m wind speed at the surface station of interest at hour h, and K is the number of surrounding soundings ($K = 5$ in this study).

[46] However, neither sounding nor surface data are available on an hourly basis for all locations. Daily averages of 10-m wind speeds at the surface stations (i.e., $\overline{V}_R$) and twice-a-day sounding profiles (at 0000 and 1200 UTC) were usually the only available data worldwide. As such, Figures 4–10 were derived by using the following equation:

$$\overline{V}80 = \frac{1}{\sum_{k=1}^{K} \frac{1}{R_k^2}} \times \sum_{k=1}^{K} \frac{1}{R_k^2} \times \frac{L_{00,k}\left(\overline{V}_R \right) + L_{12,k}\left(\overline{V}_R \right)}{2}, \qquad (18)$$

where $L_{00,k}$ and $L_{12,k}$ are calculated at sounding station k at 0000 and 1200 UTC respectively. If more than two sounding readings were available on a given day, they would all be used in equation (18) by adding their corresponding $L_{h,k}$ and dividing by the total number of profiles used; if only one sounding profile was available,

only one was used. Whether the expression in equation (18) is an accurate approximation of equation (17) cannot be established a priori, as it depends on several factors, including the diurnal variation of V10, the representativeness of the profiles at 0000 and 1200 UTC, and the time zone of each station. Observations from the KSC two-level towers were therefore used to elucidate this problem.

[47] For the 15 two-level towers, the closest five surrounding sounding stations were identified (Figure 13) and LS parameters, calculated at 0000 and 1200 UTC each day, were applied to daily averages $\overline{V}_R$ via equation (18). Results are summarized in Table 8. The application of the Steps 2 and 3 of the LS methodology, in combination with equation (18), produced good estimates of the average wind speed at the output height (16 m); at all towers, such estimates were also conservative. The average error was an underestimate of −19.8%, the worst case was −50.3% (tower 0001), and the best case was tower 0403 (−0.7%). The towers where the LS methodology performed worst (but still conservatively) were 0001, 0108, 0714, and 0303; the common factor among them was a large shear between the reference and the output wind speeds (i.e., $\rho = V^{OBS}/V^{REF}$), varying between 2.2 and 2.9. Since, from Section 2, $\rho < 3$ was a restriction imposed in the LS methodology, it is expected that such towers exhibit a larger underestimate.

[48] In summary, from the KSC tower data, an analogy can be made between sounding stations and four-level towers and another between surface stations and two-level towers. It appeared that the LS methodology performed best for sounding stations (Step 1), as the average error at four-level towers was very small (−3.3%) and negative, indicative of a conservative approach. When applied to surface stations (Steps 2 and 3), LS results were poorer (but still conservative), as the average error at two-level towers was −19.8%. Several causes can be invoked, including the distance between sounding and surface stations (Step 3), the approximation introduced by using daily averages (equation (18) instead of equation (17)), the low elevation of the "reference height" (~4 m), and the time zone of Florida (−5 from UTC), where soundings are retrieved during the diurnal/nocturnal transition. Further investigations are necessary to evaluate this. In any case, it appears that the approximation in equation (18) leads to satisfactory results.

3.2.3. Further Remarks

[49] The overall (i.e., sounding and surface stations) percent of class ≥3 stations was 12.7% (Table 1) for
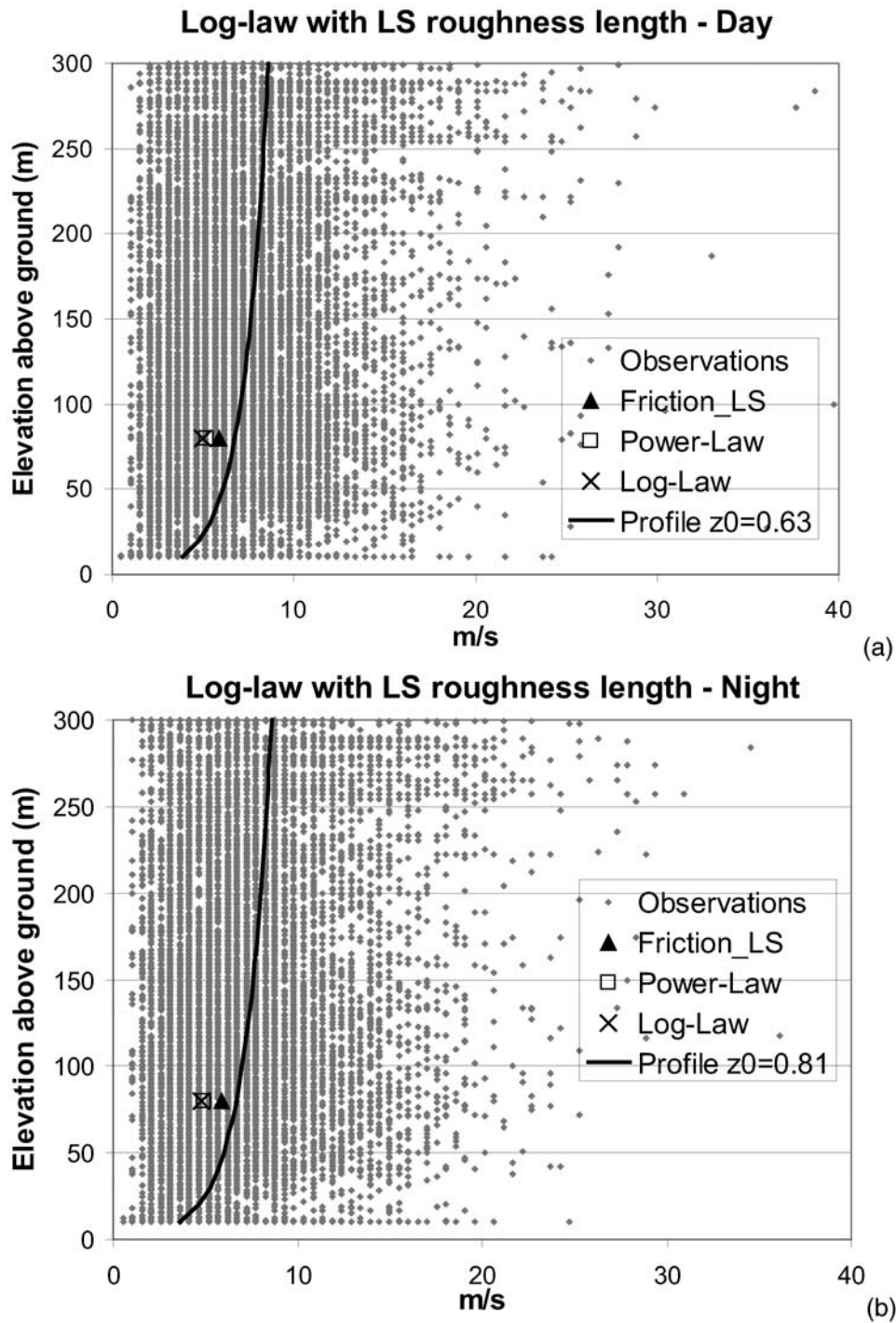
Figure 10. Wind speed observed worldwide in the lowest 300 m, calculated V80 obtained with: z_0^{LS} (triangle), $z_0 = 0.01$ (cross), $\alpha = 1/7$ (square), and profile obtained (a) with the global average $z_0^{LS} = 0.63$ (solid line) during the day and (b) with $z_0^{LS} = 0.81$ at night.

the world, and ~17% for the U.S. The latter is lower than what was found previously by *Archer and Jacobson* [2004] (22%), due to the more conservative assumptions introduced here. In fact, KSC data show that the revised LS methodology introduced in this study may underestimate 80-m wind speeds by 3–20% (Tables 7 and 8).

[50] The results of this study can be considered conservative for the following reasons. First, a comparison with the KSC tower data showed that the LS methodology gave accurate and conservative results, for both four- and two-level towers. Even though the area covered was relatively small (Figure 13), the KSC dataset included a large number of towers and its data were quality-checked prior to their
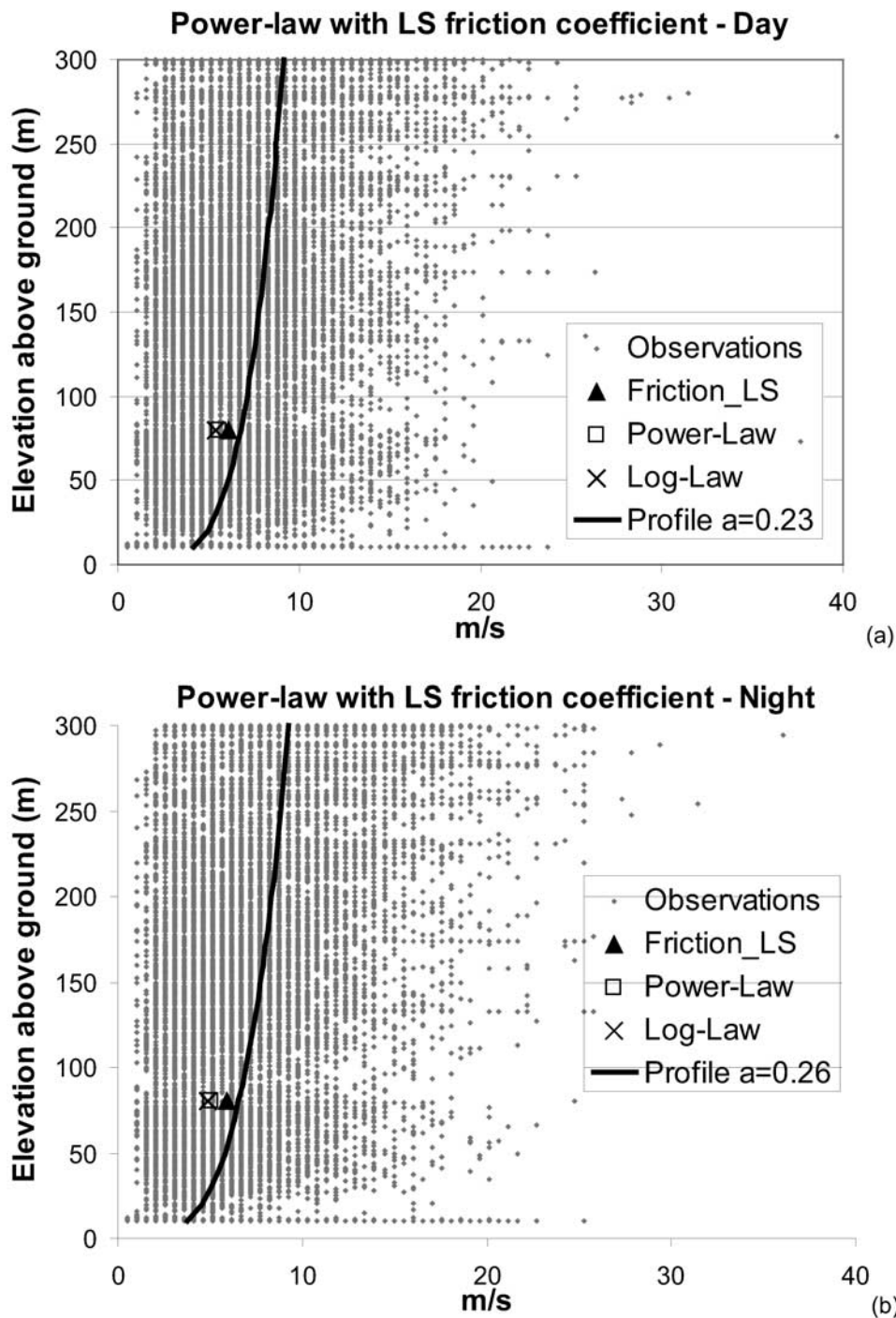
Figure 11. Wind speed observed worldwide in the lowest 300 m, calculated V80 obtained with: α^{LS} (triangle), $z_0 = 0.01$ (cross), $\alpha = 1/7$ (square), and profile obtained (a) with the world average $\alpha^{LS} = 0.23$ (solid line) during the day and (b) with $\alpha^{LS} = 0.26$ at night.

acquisition for this study. Second, remote areas with good wind power potential, but without meteorological stations, are not represented in this study. An example is the Dominican Republic, which was classified as non-suitable for wind power generation (class 1 and 2) in Figure 5. In the 1-km resolution analysis by *Elliott et al.* [2001a] showed instead substantial potential at 30 meters in the remote regions of the northwest and southwest. Similarly, Mongolia does not show

appreciable wind power potential in Figure 8, but, according to the high-resolution study by *Elliott et al.* [2001b], has been estimated to have ∼10% of land with good-to-excellent wind potential for utility-scale (i.e., at 30 m) applications. Also, countries that for political reasons do not share their meteorological data with NCDC are not represented in this study either (e.g., Laos and Iraq). Finally, the lack of data over mountain chains, which generally offer a high wind
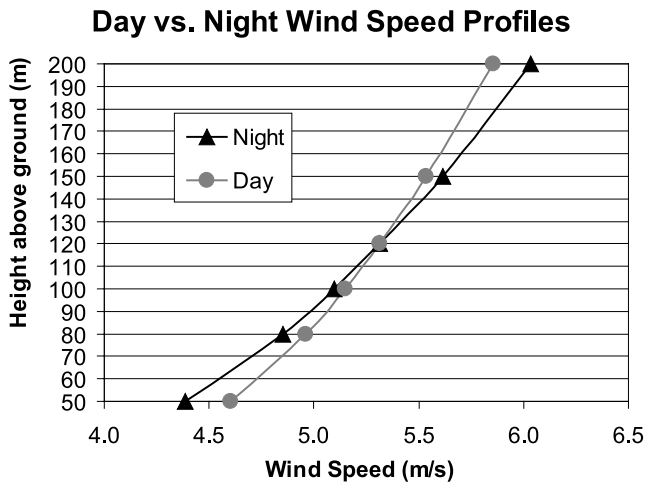
Day vs. Night Wind Speed Profiles

Figure 12. Comparison of the diurnal (diamonds) and nocturnal (squares) global average profiles of wind speed in 2000 obtained at the sounding stations (with at least 20 valid profiles) with the LS methodology for hub heights in 50–200 m.

potential but are not represented here, further suggests that the values in this study (Table 1) are conservative. Examples are: (1) the Philippines archipelago was classified as class 1 in this study (Figure 8), but it was shown to have an excellent

wind resource for utility-scale applications (at 30 meters) at mountainous and east-facing locations [*Elliott et al.*, 2001c]; (2) Armenia, represented by only one class-1 station in this study, has excellent wind power potential on top of ridges and in mountain passes [*Elliott et al.*, 2003]. Note, however, that all wind atlases cited in this study were obtained for a constant surface roughness of 0.10 m, considerable lower than the values found in the previous section (0.63–0.81 m). Also, they were valid at 30 to 50 m above ground, whereas this study focused on the 80-m hub height.

3.3. Global Wind Power

[51] In this section, the total wind power available globally for electric power generation at a direct cost of 3–4 c/kWh is estimated. The following assumptions were made for this calculation:

[52] 1. Winds are Rayleigh in nature [e.g., *Archer and Jacobson*, 2003] (Figures 10 and 11).

[53] 2. The fraction of the Earth surface covered by land (without snow) A_{land} is 25.4% [*Jacobson*, 2001], corresponding to 1.3×10^8 km^2. The fraction covered by water is 71.3%, or 3.64×10^8 km^2, and that covered by snow/ice is 3.3%, or 0.16×10^8 km^2.

[54] 3. The wind speed distribution over the globe is well represented by the wind speed distribution obtained from the 8199 stations used in this study. This is a conservative approach, as discussed in the previous sections.
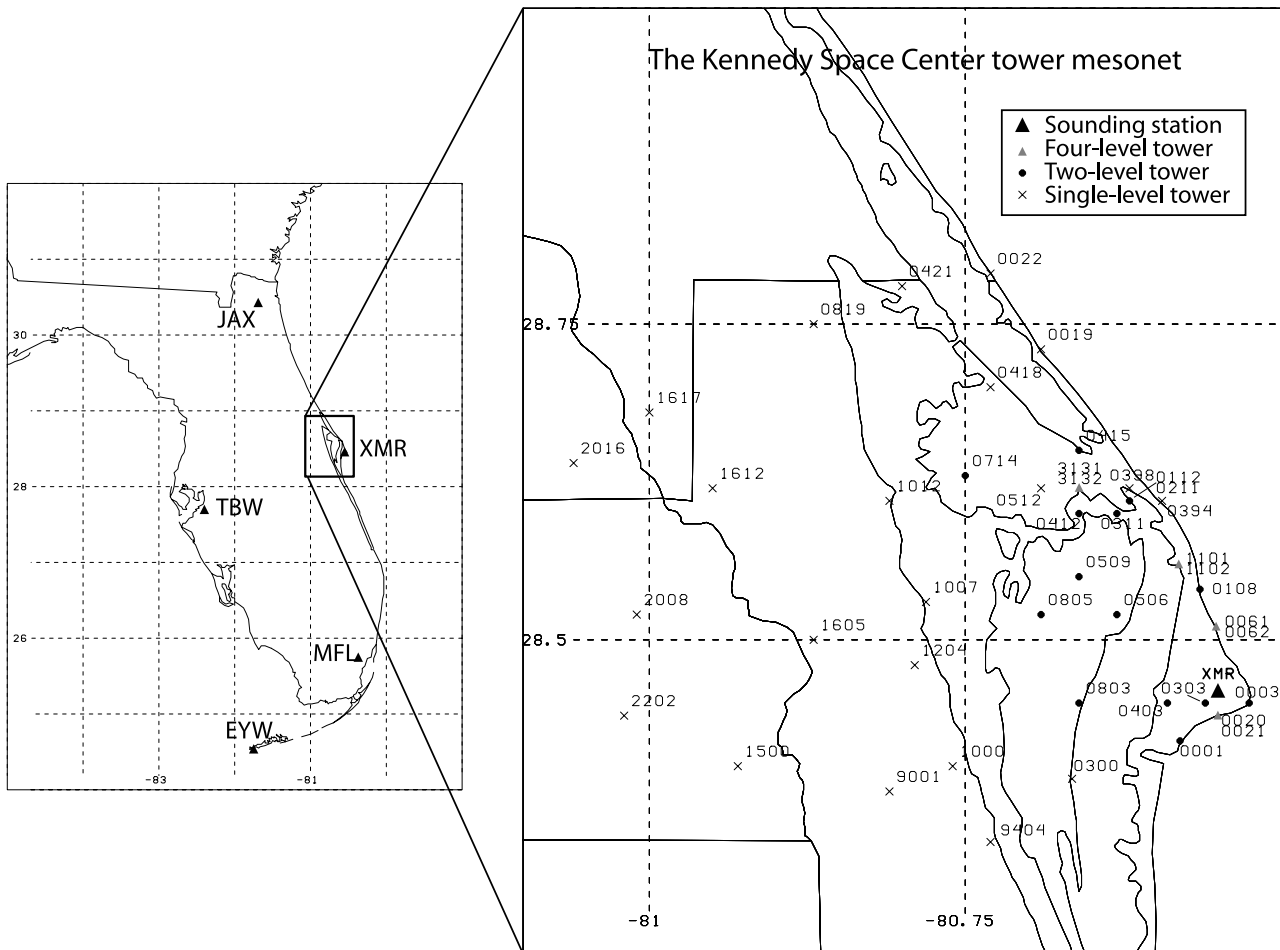

Figure 13. Location of sounding stations and towers near the Kennedy Space Center (Florida).

Table 6. List of Towers and Levels[a]

Tower ID		Levels, m						
0020	(All)	4	16 (ref)	27	44 (out)	62		
	(N = 3)		16 (ref)	27	44 (out)	62		
0021	(All)	4	16 (ref)	27	44 (out)	62		
	(N = 3)		16 (ref)	27	44 (out)	62		
0061		4 (ref)	16	49 (out)	62			
0062		4 (ref)	16	49 (out)	62			
1101		4 (ref)	16	49 (out)	62			
1102		4 (ref)	16	49 (out)	62			
3131	(All)	4	16 (ref)	49 (out)	62	90	120	150
	(N = 3)		16 (ref)	49 (out)	62			150
3132	(All)	4	16 (ref)	49 (out)	62	90	120	150
	(N = 3)		16 (ref)	49 (out)	62			150
0001		4 (ref)	16 (out)					
0003		4 (ref)	16 (out)					
0108		4 (ref)	16 (out)					
0112		4 (ref)	16 (out)					
0211		4 (ref)	16 (out)					
0303		4 (ref)	16 (out)					
0311		4 (ref)	16 (out)					
0403		4 (ref)	16 (out)					
0412		4 (ref)	16 (out)					
0415		4 (ref)	16 (out)					
0506		4 (ref)	16 (out)					
0509		4 (ref)	16 (out)					
0714		4 (ref)	16 (out)					
0803		4 (ref)	16 (out)					
0805		4 (ref)	16 (out)					

[a]The reference and the output heights are indicated with "ref" and "out," respectively.

[55] 4. The power output ($\overline{P}$, kW) from a single turbine can be obtained from:

$$\overline{P} = P_{rated} \times CF = P_{rated} \times \left[0.087\overline{V} - \frac{P_{rated}}{D^2}\right], \quad (19)$$

where P_{rated} is the rated power of the turbine (kW) and CF is the capacity factor, which can be calculated from the yearly averaged wind speed (m/s) and the turbine diameter D (m) [*Masters*, 2004; *Jacobson and Masters*, 2001]. This expression was originally derived for a specific turbine (the NEG Micon 1000 kW with D = 60 m), but it was found to be accurate to within 2.6–3.5% for a 1.5 MW, 77-m blade turbine and within a few percent of many other turbines tested. As such, these values of P_{rated} and D will be used in the rest of this study.

[56] 5. Turbine density δ is 6 turbines per km^2 for 77-m diameter turbines. This value was obtained by assuming that each turbine occupies an area of 4D × 7D = 28D^2 [*Masters*, 2004; *Jacobson and Masters*, 2001].

[57] The total power over land P_{TOT} can therefore be calculated from the fraction of stations in class ≥ 3 from Table 1 ($f_{class \geq 3} = 0.127$), the land area A_{land}, and the yearly averaged wind speed for stations in class ≥ 3 from Table 4 ($V_{class \geq 3} = 8.44$ m/s) as follows:

$$P_{TOT} = f \times A_{land} \times \delta \times \overline{P}$$
$$= 9.91 \times 10^7 \times \left[1500\,kW \times \left(0.087 \times 8.44 - \frac{1500}{77^2}\right)\right]$$
$$= 7.15 \times 10^{10}\ \text{kW} \quad (20)$$

In other words, the total wind power potential over land from class ≥ 3 areas can be estimated roughly as 72 TW, corresponding to 6.27×10^{14} kWh or, by assuming 100% primary energy equivalent and a conversion factor of 0.086 from TWh to Mtoe [*IEA*, 2003], 53898 Mtoe. Note that, from equation (20), CF = 0.48. This value may appear large, but it applies only to that portion of the land (12.7%) with high average wind speeds (class 3 or greater). Note also that, since the average 80-m wind speed used in equation (20) includes buoys and since the area between land and buoys is negligible when compared against the total land area, the global wind power estimate in this study is representative of land as well as near-shore continental-shelf areas.

[58] The global demand (or consumption) of electricity in 2001 was between 1.6 TW [*EIA*, 2004, Table 6.2] and 1.8 TW [*IEA*, 2003] ($13.8 \times 10^{12} - 15.5 \times 10^{12}$ kWh); the global demand of energy for all purposes in 2001 was between 6995 [*IEA*, 2003] and 10177 [*EIA*, 2004, Table E.1] Mtoe. (The estimates of global electricity and energy demand by *EIA* [2004] and *IEA* [2003] differ due to different accounting procedures.) As such, the amount of wind energy over land could potentially cover over five times the current global energy and about 40 times the current electricity uses with little incremental pollution. This statistic does not take into account the practicality of reaching the windy sites or of transmission (including "choke" points) or of competing land uses or of wheeling power over large distances or of switching to wind power. It is only a first estimate of available wind power.

4. Conclusions

[59] In this study, the Least Square methodology, introduced by *Archer and Jacobson* [2003] to obtain wind speeds at 80 m given only observed wind speeds at 10 m and profiler data, was revised and extended to evaluate

Table 7. Statistics of the LS Methodology Performance at Towers With at Least Four Levels of Wind Speed Data From the Kennedy Space Center Network[a]

	0020		0021		0061	0062	1101	1102	3131		3132	
	N > 3	N = 3	N > 3	N = 3	N = 3	N = 3	N = 3	N = 3	N > 3	N = 3	N > 3	N = 3
V^{OBS}, m/s	5.4	5.1	5.3	5.1	5.1	5.3	5.3	5.2	5.3	5.0	5.2	4.9
V^{LS}, m/s	5.2	5.0	5.2	5.0	4.9	5.1	5.1	5.1	5.0	4.8	5.0	4.6
V^{LOG}, m/s	4.2	4.0	4.2	4.0	2.8	2.9	3.3	3.3	4.2	3.9	4.2	3.9
V^{POW}, m/s	4.2	4.0	4.2	4.0	3.0	3.1	3.5	3.4	4.4	4.1	4.3	4.0
N. profiles	7124	7838	7820	8567	2393	2553	4888	4569	2845	3215	5556	6345
Avg ε, %	−2.6	−2.7	−1.9	−1.9	−3.4	−2.2	−2.7	−2.8	−4.8	−5.6	−3.9	−5.0
N. profiles w/ε > 50%	0	2	1	2	0	0	0	0	2	4	4	15
N. profiles w/ε < −50%	4	0	0	0	18	0	0	1	1	2	0	0
Max ε, %	28.7	61.8	370.3	383.9	21.1	14.8	48.5	44.0	113.7	123.0	129.9	139.7
Min ε, %	−93.0	−29.7	−72.2	−36.0	−77.7	−53.4	−40.9	−78.6	−52.6	−46.0	−55.1	−49.4

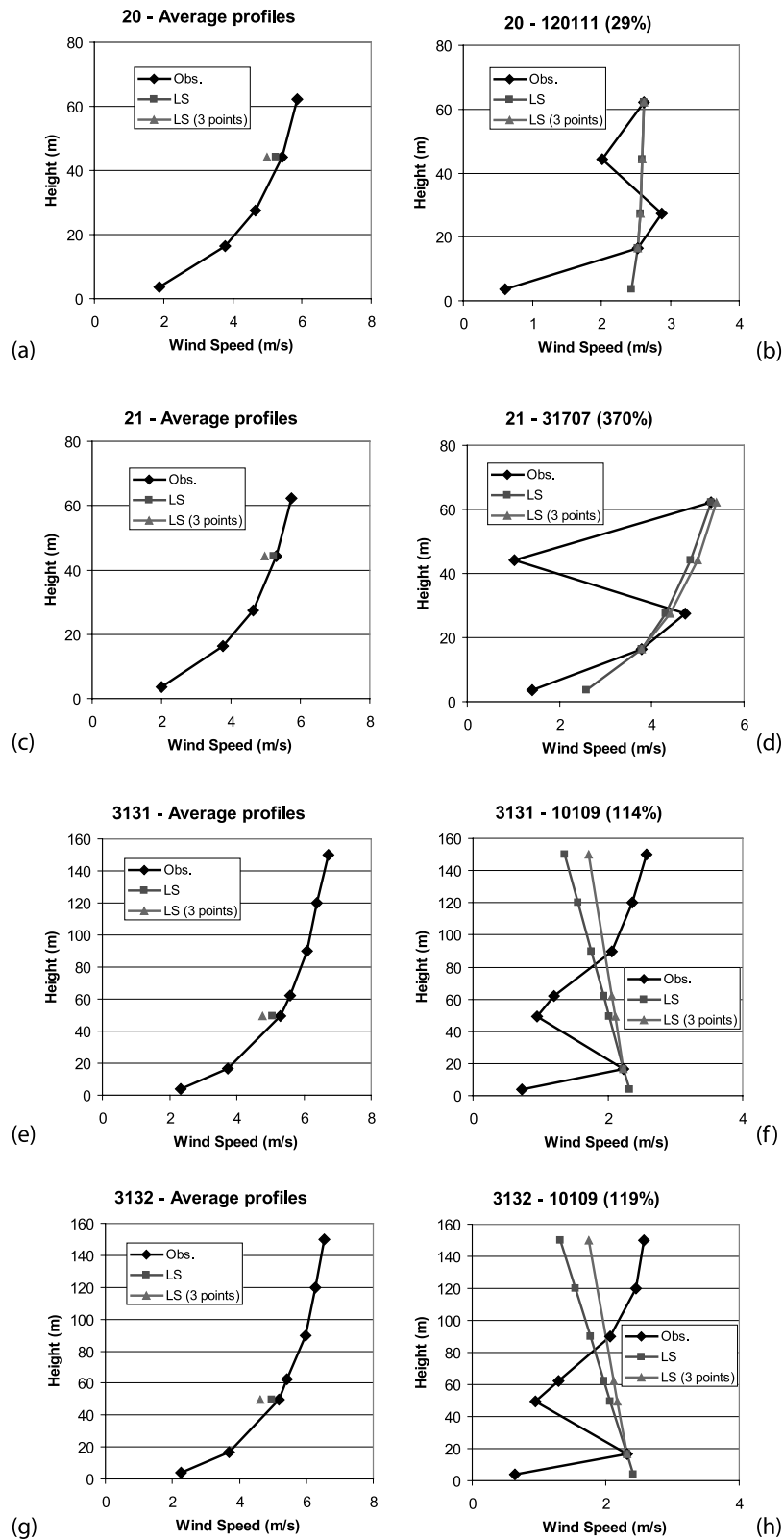[a]N is the number of levels used to calculate the LS estimates.

Figure 14. Average and worst-case profiles for towers 20, 21, 3131, and 3132.

Table 8. Statistics of the LS Methodology Performance at Two-Level Towers From the Kennedy Space Center Network

Tower ID	V^{REF}, m/s	V^{OBS}, m/s	V^{LS}, m/s	ε, %
0001	1.3	3.7	1.9	−50.3
0003	3.6	4.9	4.8	−1.8
0108	1.5	3.5	2.2	−39.4
0112	2.3	3.7	3.3	−8.1
0211	2.5	4.2	4.0	−8.9
0303	1.4	3.0	2.1	−32.2
0311	2.4	4.0	3.5	−11.5
0403	2.5	3.7	3.7	−0.7
0412	1.7	3.2	2.5	−20.1
0415	1.7	3.0	2.5	−18.1
0506	2.2	3.3	3.1	−4.6
0509	1.8	3.1	2.6	−16.7
0714	1.5	3.3	2.2	−34.5
0803	1.3	2.4	1.8	−27.6
0805	1.6	2.7	2.0	−22.6
Averages	1.9	3.4	2.8	−19.8

global wind power. The main conclusions of the study were as follows:

[60] 1. Approximately 13% of all stations worldwide belong to class 3 or greater (i.e., annual mean wind speed $\geq$ 6.9 m/s at 80 m) and are therefore suitable for wind power generation. This estimate appears to be conservative, since the application of the LS methodology to tower data from the Kennedy Space Center exhibited an average underestimate of −3.0 and −19.8% for sounding and surface stations respectively. In addition, wind power potential in all areas for which previous studies had been published was underestimated in this study.

[61] 2. The average calculated 80-m wind speed was 4.59 m/s (class 1) when all stations were included; if only stations in class 3 or higher were counted, the average was 8.44 m/s (class 5). For comparison, the average observed 10-m wind speed from all stations was 3.31 m/s (class 1) and from class $\geq$3 stations was 6.53 m/s (class 6).

[62] 3. Europe and North America have the greatest number of stations in class $\geq$ 3 (307 and 453, respectively), whereas Oceania and Antarctica have the greatest percentage (21 and 60%, respectively). Areas with strong wind power potential were found in northern Europe along the North Sea, the southern tip of the South American continent, the island of Tasmania in Australia, the Great Lakes region, and the northeastern and western coasts of Canada and the United States.

[63] 4. Offshore stations experience mean wind speeds at 80 m that are ∼90% greater than over land on average.

[64] 5. The Least Square methodology generally performed better against sounding data than did the log- and the power-laws with constant coefficients (α = 1/7 and z_0 = 0.01 m). Wind speed values predicted with the Least Square methodology were generally greater than those predicted with the constant-coefficients curves (with the exception of the linear profile, which by design predicts lower values than the constant-coefficient curves).

[65] 6. The globally averaged values of the friction coefficient α and the roughness length z_0 are 0.23–0.26 and 0.63–0.81 m, respectively. Both ranges are larger than what is generally used when no other information is available (i.e., α = 0.14 and z_0 = 0.01 m) and are more

representative of urbanized/rough surfaces than they are of grassy/smooth ones.

[66] 7. The globally averaged 80-m wind speed from the sounding stations was higher during the day (4.96 m/s) than night (4.85 m/s). Only above ∼120 m the average nocturnal wind speed was higher than the daytime average.

[67] 8. Global wind power potential for the year 2000 was estimated to be ∼72 TW (or ∼54000 Mtoe). As such, sufficient wind exists to supply all the world's energy needs (i.e., 6995–10177 Mtoe), although many practical barriers need to be overcome to realize this potential.

References

American Wind Energy Association (AWEA) (2004), Global market report 2004, Washington, D. C. (Available at http://www.awea.org/pubs/documents/globalmarket2004.pdf)

Archer, C. L. (2004), The Santa Cruz Eddy and U.S. wind power, Ph.D. thesis, 190 pp., Stanford Univ., Stanford, Calif., 1 April.

Archer, C. L., and M. Z. Jacobson (2003), Spatial and temporal distribution of U. S. winds and wind power at 80 m derived from measurements, *J. Geophys. Res.*, *108*(D9), 4289, doi:10.1029/2002JD002076.

Archer, C. L., and M. Z. Jacobson (2004), Corrections to "Spatial and temporal distribution of U. S. winds and wind power at 80 m derived from measurements," *J. Geophys. Res.*, *109*, D20116, doi:10.1029/2004JD005099.

Asia Alternative Energy Program (ASTAE) (2001), Wind energy resource atlas of Southeast Asia, Washington, D. C., Sept. (Available at http://www.worldbank.org/astae/werasa/complete.pdf)

Bolinger, M., and R. Wiser (2001), Summary of power authority letters of intent for renewable energy, memorandum, Lawrence Berkeley Natl. Lab., Berkeley, Calif., 20 Oct.

Czisch, G., and B. Ernst (2001), High wind power penetration by the systematic use of smoothing effects within huge catchment areas shown in a European example, paper presented at WINDPOWER 2001, Am. Wind Energy Assoc., Washington, D. C., June.

Elliott, D., C. G. Holladay, W. R. Barchet, H. P. Foote, and W. F. Sandusky (1986), Wind energy resource atlas of the United States, *DOE/CH 10093-4*, Dep. of Energy, Washington, D. C.

Elliott, D., M. Schwartz, R. George, S. Haymes, D. Heimiller, G. Scott, and J. Kline (2001a), Wind energy resource atlas of the Dominican Republic, *NREL/TP-500-27602*, Natl. Renewable Energy Lab., Golden, Colo., Oct.

Elliott, D., M. Schwartz, G. Scott, S. Haymes, D. Heimiller, and R. George (2001b), Wind energy resource atlas of Mongolia, *NREL/TP-500-28972*, Natl. Renewable Energy Lab., Golden, Colo., Aug.

Elliott, D., M. Schwartz, R. George, S. Haymes, D. Heimiller, G. Scott, and E. McCarthy (2001c), Wind energy resource atlas of the Philippines, *NREL/TP-500-26129*, Natl. Renewable Energy Lab., Golden, Colo., Feb.

Elliott, D., M. Schwartz, G. Scott, S. Haymes, D. Heimiller, and R. George (2002), Wind energy resource atlas of Southeast China, *NREL/TP-500-32781*, Natl. Renewable Energy Lab., Golden, Colo., Nov.

Elliott, D., M. Schwartz, G. Scott, S. Haymes, D. Heimiller, and R. George (2003), Wind energy resource atlas of Armenia, *NREL/TP-500-33544*, Natl. Renewable Energy Lab., Golden, Colo., July.

Energy Information Administration (EIA) (2004), International energy annual 2002, Dep. of Energy, Washington, D. C. (Available at http://www.eia.doe.gov/emeu/international/)

Forecast System Laboratory (FSL) (2004), *Recent Worldwide RAOB Observations* [CDROM], Boulder, Colo. (Available at http://www.fsl.noaa.gov/data/onlinedb.html)

International Energy Agency (IEA) (2003), Key world energy statistics, Paris, France. (Available at http://library.iea.org/dbtw-wpd/Textbase/nppdf/free/2003/key2003.pdf)

Jacobson, M. Z. (1999), *Fundamentals of Atmospheric Modeling*, 656 pp., Cambridge Univ. Press, New York.

Jacobson, M. Z. (2001), GATOR-GCMM: A global through urban scale air pollution and weather forecast model: 1. Model design and treatment of

soil, vegetation, roads, rooftops, water, sea ice, and snow, *J. Geophys. Res.*, *106*, 5385–5402.

Jacobson, M. Z., and G. M. Masters (2001), Exploiting wind versus coal, *Science*, *293*, 1438.

Masters, G. M. (2004), *Renewable and Efficient Electric Power Systems*, John Wiley, Hoboken, N. J., in press.

National Climatic Data Center (NCDC) (2004), *Integrated Surface Hourly Observations* [CDROM], Asheville, N. C. (Available at http://www.ncdc.noaa.gov/)

Rathmann, O. (2003), The UNDP/GEF Baltic wind atlas, *Risø-R-1402*, Risø Natl. Lab., Roskilde, Denmark, Nov.

Schwartz, M., and D. Elliott (1995), Mexico wind resource assessment project, *NREL/TP-441-7809*, Natl. Renewable Energy Lab., Golden, Colo.

Schwartz, M., and D. Elliott (2001), Remapping of the wind energy resource in the Midwestern United States, *NREL/AB-500-31083*, Natl. Renewable Energy Lab., Golden, Colo.

Starkov, A. N., L. Landberg, P. P. Bezroukikh, and M. M. Borisenko (2000), Russian wind atlas, 551 pp., Russ.-Dan. Inst. for Energy Efficiency, Moscow, Russia.

Troen, I., and E. L. Petersen (1989), European wind atlas, 656 pp., Risø Natl. Lab., Roskilde, Denmark.

————————————

C. L. Archer and M. Z. Jacobson, Department of Civil and Environmental Engineering, Stanford University, Stanford, CA 94305, USA. (lozej@stanford.edu)